Design Principle for Decoding Calcium Signals to Generate Specific Gene Expression Via Transcription[1]

Junli Liu,[a,2] Gioia Lenzoni,[b] and Marc R. Knight[a,2,3]

[a]Department of Biosciences, Durham University, Durham DH1 3LE, United Kingdom
[b]School of Pharmaceutical Sciences, University of Geneva, Geneva CH-1211, Switzerland

ORCID IDs: 0000-0001-8264-2450 (J.L.); 0000-0002-2367-6834 (G.L.); 0000-0002-4830-8608 (M.R.K.).

The second messenger calcium plays a key role in conveying specificity of signaling pathways in plant cells. Specific calcium signatures are decoded to generate correct gene expression responses and amplification of calcium signatures is vital to this process. (1) It is not known if this amplification is an intrinsic property of all calcium-regulated gene expression responses and whether all calcium signatures have the potential to be amplified, or (2) how a given calcium signature maintains specificity in cells containing a great number of transcription factors (TFs) and other proteins with the potential to be calcium-regulated. The work presented here uncovers the design principle by which it is possible to decode calcium signals into specific changes in gene transcription in plant cells. Regarding the first question, we found that the binding mechanism between protein components possesses an intrinsic property that will nonlinearly amplify any calcium signal. This nonlinear amplification allows plant cells to effectively distinguish the kinetics of different calcium signatures to produce specific and appropriate changes in gene expression. Regarding the second question, we found that the large number of calmodulin (CaM)-binding TFs or proteins in plant cells form a buffering system such that the concentration of an active CaM-binding TF is insensitive to the concentration of any other CaM-binding protein, thus maintaining specificity. The design principle revealed by this work can be used to explain how any CaM-binding TF decodes calcium signals to generate specific gene expression responses in plant cells via transcription.

Plants are sessile organisms and therefore they must adapt their metabolism, growth, and architecture to a changing environment. To survive, it is vital for plants to be able to sense and act upon environmental information. Central to this are "second messengers": cellular chemicals that convey information from the outside world to the cells that make up a plant. Second messengers have evolved to trigger the required response of cells to environmental cues. Calcium is a ubiquitous second messenger for activating tolerance mechanisms in plants responding to environmental stresses (McAinsh et al., 1995; Allen et al., 2001; Love et al., 2004; Miwa et al., 2006; McAinsh and Pittman, 2009; Dodd et al., 2010; Short et al., 2012; Edel et al., 2017; Yuan et al., 2017; Bender et al., 2018; Kudla et al., 2018).

The majority of plant defense responses against stress are realized by changes in gene expression to produce proteins required to combat the conditions they encounter. It is thus vital that the correct proteins are produced in response to different environmental conditions, i.e. different genes need to be switched on in response to different stimuli. This means that the identity of the primary stimulus must be encoded in a language that the cell can understand. Most stimuli lead to transient elevation in cellular calcium levels. Importantly, different stimuli produce calcium elevations with different characteristics: a unique calcium signature. Consequently, the specific properties of different calcium signatures have been proposed to encode information on the identity of the stimulus (McAinsh et al., 1995; Allen et al., 2001; Love et al., 2004; Miwa et al., 2006; McAinsh and Pittman, 2009; Dodd et al., 2010; Short et al., 2012)

Experimental data showed that calcium signals can be decoded to generate specific gene expression responses (Whalley et al., 2011; Whalley and Knight, 2013), and modeling analysis revealed that amplification of calcium signals is important for decoding calcium signals (Liu et al., 2015; Lenzoni et al., 2018). However, it remains unclear whether decoding calcium signatures in plant cells is governed by any general principle.

The complexity for plant cells to decode specific calcium signatures is multifaceted. First, any, even a modest, calcium signature (e.g. in response to ozone; Clayton et al., 1999) is able to induce gene expression. Second, the specific characteristics of the calcium signatures produced by different stresses encode stimulus-specific information. Experimental

[1]This work was supported by the European Research Council (CALIPSO GA 2013-607607 to G.L.)

[2]Senior authors.

[3]Author for contact: m.r.knight@durham.ac.uk.

The author responsible for distribution of materials integral to the findings presented in this article in accordance with the policy described in the Instructions for Authors (www.plantphysiol.org) is: Marc R. Knight (m.r.knight@durham.ac.uk).

M.R.K. and J.L. conceived the project and original research plans; M.R.K. supervised the experiments; G.L. performed most of the experiments; J.L. performed the modelling analysis; M.R.K. and J.L. wrote the article with contributions of all the authors.

www.plantphysiol.org/cgi/doi/10.1104/pp.19.01003

evidence demonstrates that Arabidopsis (*Arabidopsis thaliana*) is able to decode specific calcium signatures and interpret them, leading to distinct gene expression profiles (Whalley et al., 2011; Whalley and Knight, 2013). Third, a variety of experimental data show that there are a large number of calmodulin (CaM)-binding proteins (Reddy et al., 2011; Poovaiah et al., 2013; Virdi et al., 2015; Edel et al., 2017; Yuan et al., 2017; Bender et al., 2018; Kudla et al., 2018). CaM has two pairs of Ca^{2+}-binding EF-hand domains located at the N- and C-termini, respectively (Finn and Forsén, 1995; Valeyev et al., 2008). Some transcription factors (TFs) can bind to Ca^{2+}-CaM, allowing them to respond to calcium signals via this Ca^{2+}–CaM–TF interaction. Clearly, for TFs to decode calcium signals, and therefore generate specific gene expression responses, they must be able to distinguish the kinetics of different calcium signals in the context of competing for binding CaM with other CaM-binding proteins. However, how this occurs is unknown. In general, the search for basic underlying principles is vital for a better understanding of the regulation of signaling dynamics. Cells navigate environments and communicate and build complex patterns by initiating specific gene expression responses to specific signals (Brophy and Voigt, 2014). Studies in other cellular systems (Savageau, 2001; Salvador and Savageau, 2003, 2006; Wall et al., 2003; Purvis and Lahav, 2013; Tolla et al., 2015; Karin et al., 2016) have found that biological networks may be evolutionarily tuned and regulatory architecture of a biological network is optimized following some basic principles underlying evolutionary selection (Salvador and Savageau, 2003; Chubukov et al., 2012). Design principles are the underlying properties of network structures that have evolved to endow the network functions. Although experimental data showed that calcium signals can be decoded to generate specific gene expression responses (Whalley et al., 2011; Whalley and Knight, 2013) and modeling analysis revealed that amplification of calcium signals is important for decoding calcium signals (Liu et al., 2015; Lenzoni et al., 2018), it remains unclear whether decoding calcium signatures in plant cells is governed by any general principle. This work uncovers the design principle for decoding calcium signals through changes in transcription by addressing the following questions: Is amplification of Ca^{2+} signatures an intrinsic property of all calcium-regulated gene expression responses, and do all calcium signatures have the potential to be amplified? And how does decoding of calcium signals maintain specificity when one messenger (Ca^{2+}) is decoded by many TFs and proteins in plant cells? This work establishes the link between the characteristics of CaM (i.e. it has two pairs of Ca^{2+}-binding EF-hand domains and it is capable of binding a large number of proteins in plant cells) with the intrinsic properties of Ca^{2+}–CaM–TF interactions, to reveal the design principle underpinning how plant cells decode calcium signals to generate specific gene expression response via changes in transcription. We show that both a theoretical simple gene expression system and an empirical system of two plant immunity genes (*enhanced disease susceptibility1* [*EDS1*] and *isochorismate synthase1* [*ICS1*]; Lenzoni et al., 2018) follow this design principle to decode calcium signatures. The principle revealed in this work is applicable to study how any CaM-binding TF decodes calcium signals to generate specific gene expression response in plant cells via transcription.

RESULTS

Amplification of Calcium Signal Is an Intrinsic Property of Ca^{2+}–CaM–TF Interactions

The interaction of Ca^{2+}, CaM, and another (CaM-binding) protein can form many different binding complexes. CaM has two pairs of Ca^{2+}-binding EF-hand domains located at the N- and C-termini, respectively (Finn and Forsén, 1995; Valeyev et al., 2008). Experimental measurement showed that $4Ca^{2+}$–CaM is the active CaM–Ca^{2+} binding complex (Pifl et al., 1984). Therefore, this work assumes that the $4Ca^{2+}$–CaM–TF complex is the active complex for gene expression responses. The cooperative binding between Ca^{2+} and the four binding sites of CaM has previously been subjected to both experimental and modeling studies (Fajmut et al., 2005; Shifman et al., 2006; Pepke et al., 2010; Liu et al., 2015) and the kinetic parameters have been experimentally determined (Shifman et al., 2006; Pepke et al., 2010).

For any TF with one CaM-binding site, 18 different binding complexes can form via 33 elementary binding processes (Supplemental Text). For example, the binding among Ca^{2+}, CaM, and CaM-binding transcription activators (CAMTAs), and the binding among Ca^{2+}, CaM, and CaM-binding protein 60g (CBP60g) have been previously described in detail (Liu et al., 2015; Lenzoni et al., 2018). For any CaM-binding TF, and following the previous analysis (Liu et al., 2015), there are six adjustable parameters for fully examining the dynamics of Ca^{2+}–CaM–TF interactions after using the experimentally determined parameters and introducing basic thermodynamic constraints. P describes the cooperative binding between CaM and a TF in the presence of Ca^{2+}. $P > 1$, $P = 1$, or $P < 1$ represents the binding affinity of Ca^{2+}–CaM complex to the TF being looser than, the same as, or tighter than binding of free CaM to the TF, respectively. K_{14} is the dissociation equilibrium constant for the binding of the Ca^{2+}–CaM complex to the transcription factor. The term $k_{on(14)}$ is the on-rate for the binding of Ca^{2+}–CaM complex to the TF; Q describes how the cooperative binding between CaM and the TF in the presence of Ca^{2+} is realized by k_{on}, k_{off}, or both. $[CaM_t]$ describes the total concentration of CaM, which is the summation of free CaM and all CaM complexes. $[TF_t]$ describes the total concentration of the TF, which is the summation of free TF and all TF complexes.

Here we consider that a "quasi-equilibrium state" is established for Ca^{2+}–CaM–TF interactions according to the detailed balance principle (Alberty, 2004). Establishing a quasi-equilibrium state requires the on- and off-rates for all binding reactions of Ca^{2+}–CaM–TF interactions are relatively fast so that each reaction can establish an equilibrium. In the sections "Case Study 1: A Simple Ca^{2+}-Regulated Gene Expression System" and "Case Study 2: Plant Immunity Gene Expression," we will show that this assumption is valid for experimentally measured parameters of Ca^{2+}–CaM–TF interactions. At a quasi-equilibrium state, $k_{on(14)}$ and Q become irrelevant. Thus, there are only four adjustable parameters (i.e. P, K_{14}, $[CaM_t]$, and $[TF_t]$) for examining the dynamics of Ca^{2+}–CaM–TF interactions.

At a quasi-equilibrium state and for any calcium concentration, the concentration of each Ca^{2+}–CaM–TF complex can be analytically derived (Supplemental Text). Equation 1 shows the concentration of the active complex, $4Ca^{2+}$–CaM–TF:

$$[4Ca^{2+}-CaM-TF]=\frac{\frac{[CaM_t][Ca^{2+}]^4[TF]}{K_1K_2K_3K_4K_{14}}}{1+\frac{P[TF]}{K_{14}}+\left(1+\frac{[TF]}{K_{14}}\right)\left(\frac{[Ca^{2+}]}{K_1}+\frac{[Ca^{2+}]}{K_3}+\frac{[Ca^{2+}]^2}{K_1K_2}+\frac{[Ca^{2+}]^2}{K_1K_3}+\frac{[Ca^{2+}]^2}{K_3K_4}+\frac{[Ca^{2+}]^3}{K_1K_2K_3}+\frac{[Ca^{2+}]^3}{K_1K_3K_4}+\frac{[Ca^{2+}]^4}{K_1K_2K_3K_4}\right)} \quad (1)$$

K_1, K_2, K_3, and K_4 are the dissociation equilibrium constants for binding of first and second Ca^{2+} to the CaM C terminus, and for binding of first and second Ca^{2+} to the CaM N terminus, respectively. [TF] is the concentration of the free transcription factor, and it can be calculated using the total concentration of the transcription factor and the concentrations of all CaM-TF complexes. Other symbols in Equation 1 are as described above.

At an unperturbed cellular state where a calcium signature has not yet emerged, the calcium concentration settles onto a steady-state value, $[Ca^{2+}]_{ss}$. In this state, expression of a gene, which is regulated by the active signal, $4Ca^{2+}$–CaM–TF, is at a fixed level, corresponding to $[Ca^{2+}]_{ss}$. Kinetics of different calcium signatures have different temporally changing features of calcium concentration. Due to the innate properties of the Ca^{2+}–CaM–TF interactions, different calcium signatures are decoded into different temporally changing concentrations of the active complex, $4Ca^{2+}$–CaM–TF, which in turn regulates gene expression. Thus, the first step for elucidating the information flow from a calcium signal to a specific gene expression response is to examine how the signal is decoded into a temporally changing concentration of the active signal, $[4Ca^{2+}-CaM-TF]$.

Equation 2 describes the ratio of $[4Ca^{2+}-CaM-TF]$ for any $[Ca^{2+}]$ to that for $[Ca^{2+}]_{ss}$,

$$\frac{[4Ca^{2+}-CaM-TF]}{[4Ca^{2+}-CaM-TF]_{ss}}=\left(\frac{[Ca^{2+}]}{[Ca^{2+}]_{ss}}\right)^4 f=\left(\frac{[Ca^{2+}]}{[Ca^{2+}]_{ss}}\right)^4\frac{g_{ss}+P+\frac{K_{14}}{[TF]_{ss}}(1+g_{ss})}{g+P+\frac{K_{14}}{[TF]}(1+g)}$$

with

$$f=\frac{\frac{1}{[TF]_{ss}}+\frac{P}{K_{14}}+\left(\frac{1}{[TF]_{ss}}+\frac{1}{K_{14}}\right)\left(\frac{[Ca^{2+}]_{ss}}{K_1}+\frac{[Ca^{2+}]_{ss}}{K_3}+\frac{[Ca^{2+}]_{ss}^2}{K_1K_2}+\frac{[Ca^{2+}]_{ss}^2}{K_1K_3}+\frac{[Ca^{2+}]_{ss}^2}{K_3K_4}+\frac{[Ca^{2+}]_{ss}^3}{K_1K_2K_3}+\frac{[Ca^{2+}]_{ss}^3}{K_1K_3K_4}+\frac{[Ca^{2+}]_{ss}^4}{K_1K_2K_3K_4}\right)}{\frac{1}{[TF]}+\frac{P}{K_{14}}+\left(\frac{1}{[TF]}+\frac{1}{K_{14}}\right)\left(\frac{[Ca^{2+}]}{K_1}+\frac{[Ca^{2+}]}{K_3}+\frac{[Ca^{2+}]^2}{K_1K_2}+\frac{[Ca^{2+}]^2}{K_1K_3}+\frac{[Ca^{2+}]^2}{K_3K_4}+\frac{[Ca^{2+}]^3}{K_1K_2K_3}+\frac{[Ca^{2+}]^3}{K_1K_3K_4}+\frac{[Ca^{2+}]^4}{K_1K_2K_3K_4}\right)}$$

and

$$g_{ss}=\frac{[Ca^{2+}]_{ss}}{K_1}+\frac{[Ca^{2+}]_{ss}}{K_3}+\frac{[Ca^{2+}]_{ss}^2}{K_1K_2}+\frac{[Ca^{2+}]_{ss}^2}{K_1K_3}+\frac{[Ca^{2+}]_{ss}^2}{K_3K_4}+\frac{[Ca^{2+}]_{ss}^3}{K_1K_2K_3}+\frac{[Ca^{2+}]_{ss}^3}{K_1K_3K_4}+\frac{[Ca^{2+}]_{ss}^4}{K_1K_2K_3K_4}$$

$$g=\frac{[Ca^{2+}]}{K_1}+\frac{[Ca^{2+}]}{K_3}+\frac{[Ca^{2+}]^2}{K_1K_2}+\frac{[Ca^{2+}]^2}{K_1K_3}+\frac{[Ca^{2+}]^2}{K_3K_4}+\frac{[Ca^{2+}]^3}{K_1K_2K_3}+\frac{[Ca^{2+}]^3}{K_1K_3K_4}+\frac{[Ca^{2+}]^4}{K_1K_2K_3K_4} \quad (2)$$

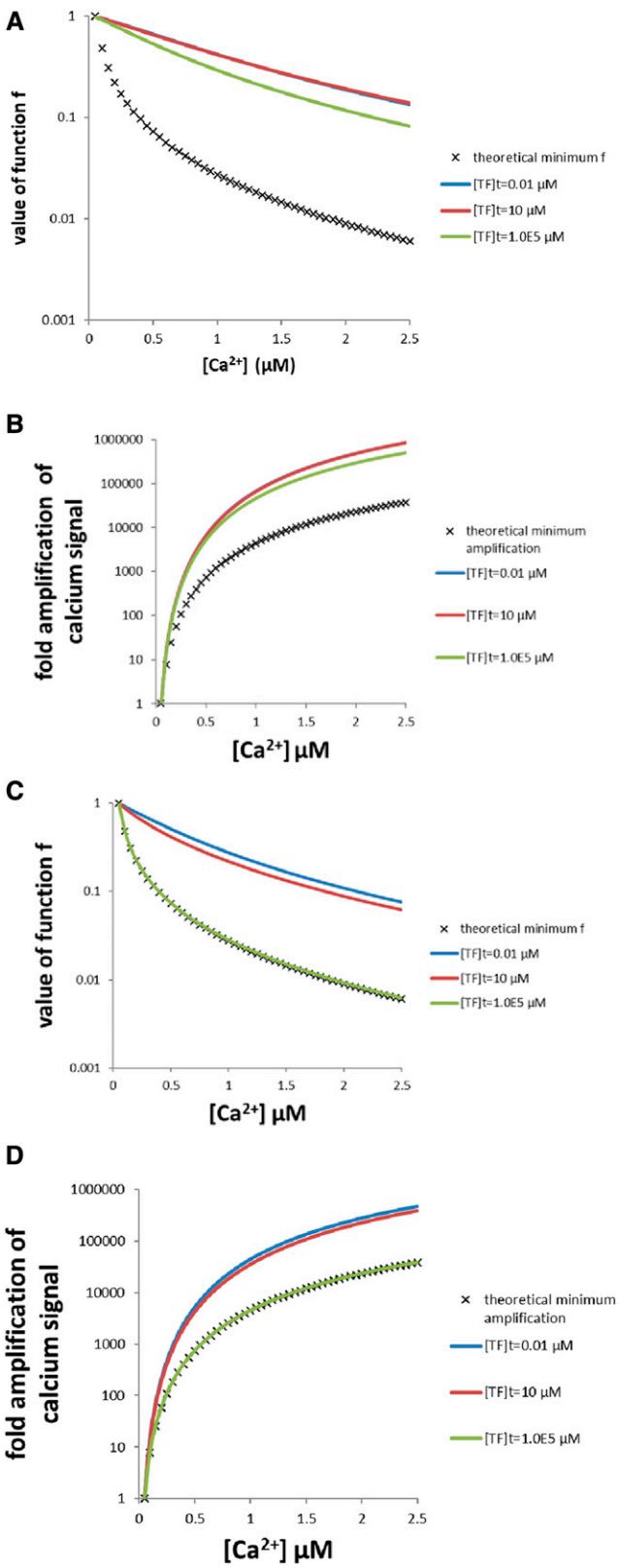

Figure 1. Ca^{2+}–CaM–TF interactions always amplify calcium signals. The parameter for the cooperative binding between CaM and a TF in the presence of Ca^{2+} is *P*. A, Value of function *f* for $P = 0.1$. Scatter crosses are the theoretical minimum value of *f*. The blue, red, and green curves correspond to the total concentration of TF, $[TF_t]$, to be 0.01, 10, and 1.0e5 μM, respectively. The blue and red curves overlap, indicating that the numerical values of *f* are always the same for the two concentrations of TF. B, Corresponding to (A), $\frac{[4Ca^{2+} - CaM - TF]}{[4Ca^{2+} - CaM - TF]_{ss}}$ value for $P = 0.1$ is calculated using Equation 2. C, Value of function *f* for $P = 1.0e\text{-}4$. Blue, red, and green curves correspond to total concentration of TF, $[TF_t]$, to be 0.01, 10, and 1.0e5 μM, respectively. The green curve and the scatter crosses overlap, indicating that the numerical values of *f* for $[TF_t] = 1.0e5$ μM are always the same as the theoretical minimum value of *f*. D, Corresponding to (C), the $\frac{[4Ca^{2+} - CaM - TF]}{[4Ca^{2+} - CaM - TF]_{ss}}$ value for $P = 1.0E\text{-}4$ is calculated using Equation 2.

Equation 2 shows that, at any calcium concentration, the fold change of calcium signal is always amplified by the power of 4, $\left(\frac{[Ca^{2+}]}{[Ca^{2+}]_{ss}}\right)^4$, multiplied by a modification term, *f*. To estimate the magnitude of this amplification, we need to estimate the lower limit of *f*. First, *f* has the following property. The term *f* is always <1, and it decreases when $[Ca^{2+}]$ increases. This is because increasing $[Ca^{2+}]$ increases term *g* and simultaneously decreases the concentration of the free transcription factor, [TF], for a constant total concentration of the transcription factor $[TF_t]$. Second, the value of *f* is dependent on both $[TF]_{ss}$ and [TF], both of which increase with $[TF_t]$. In plant cells, a typical calcium signature can increase cytosolic calcium concentration from its steady-state concentration (~0.05 μM) to up to 2.5 μM with contrastingly different kinetics (Knight et al., 1996, 1997; Aslam et al., 2008). If we consider that, within this range of $[Ca^{2+}]$, the free TF concentration is only determined by the total concentration of the TF, we are able to deduce that the lower limit of *f* is $\frac{g_{ss}}{g}$ (Supplemental Text), namely *f* is always larger than $\frac{g_{ss}}{g}$. Thus, when $[Ca^{2+}]$ increases from $[Ca^{2+}]_{ss}$ to $[Ca^{2+}]$, the minimum amplification of the calcium signal into the active signal, $\frac{[4Ca^{2+} - CaM - TF]}{[4Ca^{2+} - CaM - TF]_{ss}}$, is $\left(\frac{[Ca^{2+}]}{[Ca^{2+}]_{ss}}\right)^4 \frac{g_{ss}}{g}$.

To determine the values of $\left(\frac{[Ca^{2+}]}{[Ca^{2+}]_{ss}}\right)^4 \frac{g_{ss}}{g}$, we need the values of the four parameters (K_1, K_2, K_3, and K_4). These four parameters have been experimentally determined and their values are $K_1 = 10$ μM, $K_2 = 0.925$ μM, $K_3 = 25$ μM, and $K_4 = 5$ μM (Linse et al., 1991; Shifman et al., 2006; Kubota et al., 2007; Pepke et al., 2010). To show the ability of Ca^{2+}–CaM–TF interaction to amplify a calcium signal, we analyzed an example, for which $[Ca^{2+}]$ increases to 2.5 μM from its steady-state value of 0.05 μM. For $[Ca^{2+}]_{ss} = 0.05$ μM, $g([Ca^{2+}]_{ss}, K) = 0.0073$. When $[Ca^{2+}]$ increases to 0.25 μM (i.e. 5-fold), 0.5 μM (i.e. 10-fold), 1.0 μM (i.e. 20-fold), and 2.5 μM (i.e. 50-fold), the minimum amplification of these calcium concentrations into the concentrations of their active signals, $\frac{[4Ca^{2+} - CaM - TF]}{[4Ca^{2+} - CaM - TF]_{ss}}$, is 107-fold,

725-fold, 4,390-fold, and 37,570-fold, respectively. Thus, the Ca^{2+}–CaM–TF interaction possesses an intrinsic property of nonlinearly amplifying any calcium signal, which is quantitatively described by Equation 2.

Figure 1 shows the numerical results that confirm the above theoretical analysis for a wide range of total concentrations of a TF (0.01 μM to 1.0e5 μM). Figure 1A shows that f is always <1, that increasing $[Ca^{2+}]$ decreases the value of f, and that f is always larger than $\frac{g_{ss}}{g}$. Figure 1B shows that the term f is relatively unimportant and any calcium signal is always amplified. Therefore, numerical analysis confirms theoretical analysis: A calcium signal is always amplified due to Ca^{2+}–CaM–TF interaction. In addition, after the derivation of the lower limit of f in the Supplemental Text, we know that decreasing the parameter for the cooperative binding between CaM and a TF in the presence of Ca^{2+}, P (Liu et al., 2015; Lenzoni et al., 2018), or increasing the concentration of the TF, decreases the value of f. Figure 1 shows that numerical results are in agreement with theoretical analysis. When P is sufficiently small and $[TF_t]$ is sufficiently large, fold amplification of calcium signal is the same as the theoretical minimal fold amplification (Fig. 1, B and D).

Based on the above analysis, it can be seen that any calcium signal is always amplified by the power of 4 of calcium concentration ratio, $\left(\frac{[Ca^{2+}]}{[Ca^{2+}]_{ss}}\right)^4$, multiplied by a factor that is relatively less important, $\frac{g_{ss}}{g}$. In Equation 2, the main factor for amplifying a calcium signal is the term $\left(\frac{[Ca^{2+}]}{[Ca^{2+}]_{ss}}\right)^4$. Derivation of Equation 2 reveals that the term $\left(\frac{[Ca^{2+}]}{[Ca^{2+}]_{ss}}\right)^4$ emerges from two pairs of Ca^{2+}-binding EF-hand domains and a TF-binding domain in the CaM structure. Therefore, the ability of CaM to bind four Ca^{2+} and one TF molecule results in the amplification of calcium signal. In other words, the Ca^{2+}–CaM–TF binding mechanism naturally leads to amplification of calcium signals. As we will show below, this aspect of the underlying design principle, which links the Ca^{2+}–CaM–TF binding mechanism with the emerging property of calcium signal amplification, leads to preferential expression of specific calcium-regulated genes.

Concentration of a CaM-Binding TF-Specific Active Signal Is Insensitive to Changes in Concentration of Other CaM-Binding Proteins

A variety of experimental data show that there are a large number of CaM-binding proteins in plant cells (Reddy et al., 2011; Poovaiah et al., 2013; Virdi et al., 2015). Thus, when a calcium signature emerges, a specific TF must compete for the binding of CaM with other CaM-binding proteins. An important question, therefore, is how is a CaM-binding TF capable of generating a specific gene expression response by decoding a calcium signature in the context of competing for CaM binding with many other CaM-binding proteins? To address this question, the effects of the existence of a large number of CaM-binding proteins on the concentration of a CaM-binding TF-specific active signal must be examined.

When many proteins compete for the binding of CaM, the concentration of the active complex of a transcription factor (TF_i), $4Ca^{2+}$–CaM–TF_i, can be derived following the method used for deriving Equation 1 and is described by Equation 3:

$$[4Ca^{2+} - CaM - TF_i] = \frac{\frac{[CaM_t][Ca^{2+}]^4[TF_i]}{K_1K_2K_3K_4K_{i,14}}}{1 + \sum_{j=1}^{n}\frac{P_j[TF_j]}{K_{j,14}} + \left(1 + \sum_{j=1}^{n}\frac{[TF_j]}{K_{j,14}}\right)\left(\frac{[Ca^{2+}]}{K_1} + \frac{[Ca^{2+}]}{K_3} + \frac{[Ca^{2+}]^2}{K_1K_2} + \frac{[Ca^{2+}]^2}{K_1K_3} + \frac{[Ca^{2+}]^2}{K_3K_4} + \frac{[Ca^{2+}]^3}{K_1K_2K_3} + \frac{[Ca^{2+}]^3}{K_1K_3K_4} + \frac{[Ca^{2+}]^4}{K_1K_2K_3K_4}\right)} \quad (3)$$

Here, TF_i and TF_j are the free form of the ith and jth TF, respectively; P_j is the parameter for quantifying the cooperative binding between CaM and TF_j in the presence of Ca^{2+}; $K_{i,14}$ and $K_{j,14}$ are the dissociation equilibrium constants for the binding of Ca^{2+}–CaM complex to TF_i and TF_j, respectively; and n is the total number of CaM-binding proteins. In Equation 3, for simplifying notations, TF_j can be any TF or protein that binds with CaM. Therefore, following Equation 3, the existence of any CaM-binding TF or protein, TF_j, could affect the concentration of the active complex of a transcription factor TF_i, $4Ca^{2+}$–CaM–TF_i, by competing for the binding of CaM with TF_i. In Equation 3, this competition is described by the two summation terms: $\sum_{j=1}^{n}\frac{P_j[TF_j]}{K_{j,14}}$ and $\sum_{j=1}^{n}\frac{[TF_j]}{K_{j,14}}$.

We consider that the total concentration of CaM is $[CaM]_t$ and the concentration of each of the CaM-binding proteins, TF_j, is $[TF_j]_t$ ($j = 1,\ldots n$). When many proteins compete for the binding of CaM, the following constraints must apply. The concentration summation of free CaM and all CaM complexes with different proteins must be equal to $[CaM]_t$ at any calcium concentration. The total concentration for any TF is the concentration summation of free protein, TF_j, and all TF_j-binding complexes $[TF_j]_t$ at any calcium concentration.

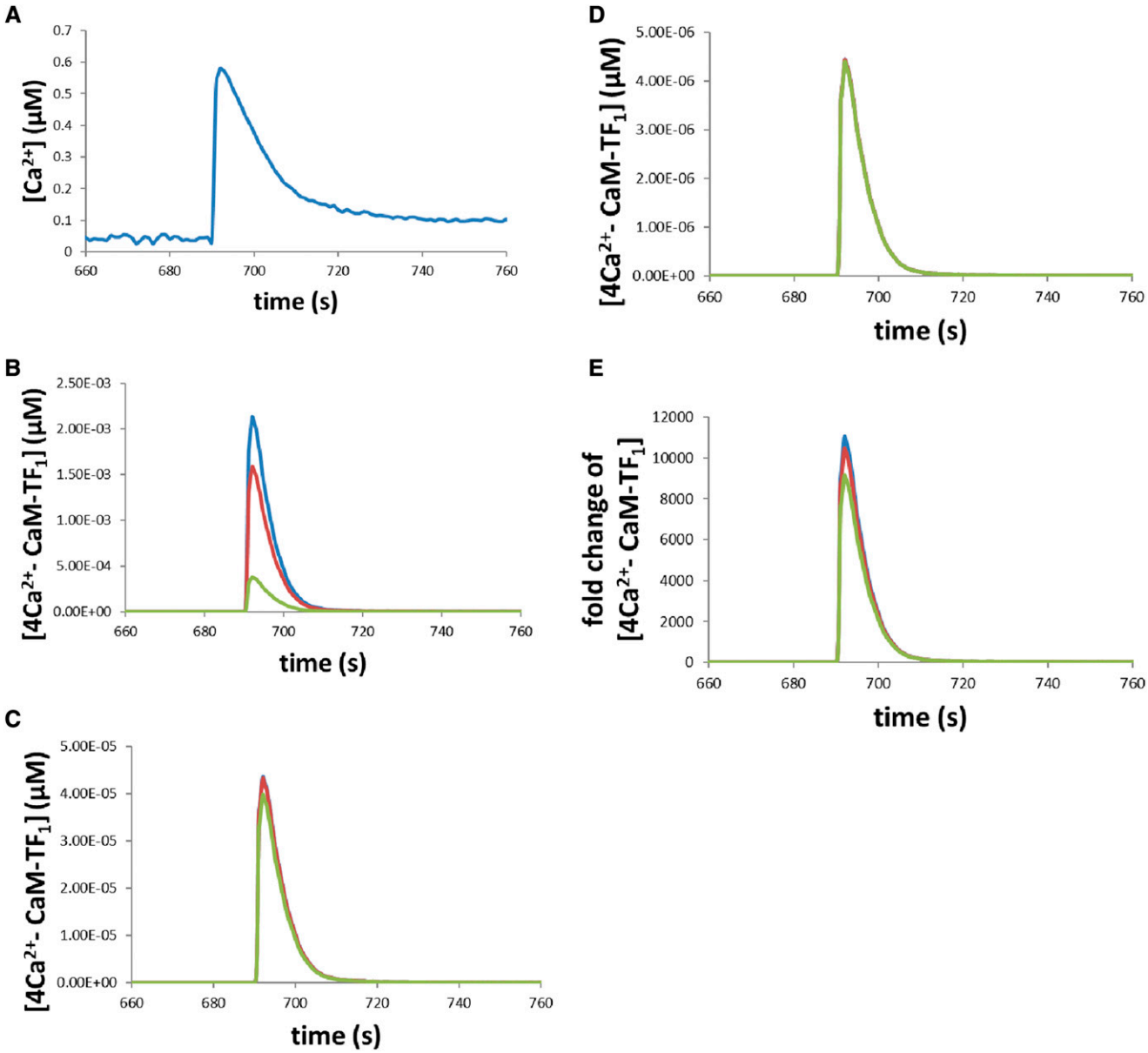

Figure 2. Effects of changing the concentration of a CaM-binding protein on the concentration of a CaM-binding TF-specific active signal when the TF and different numbers of CaM-binding proteins coexist. A, An experimentally measured calcium signature (Whalley et al., 2011). The calcium signature is used to calculate $[4Ca^{2+} - CaM - TF]$ following Equation 3. B, The TF coexists with one protein. The blue, red, and green curves correspond to the concentration of the protein to be 1, 10, and 100 μM, respectively. C, The TF coexists with 11 proteins. Concentrations of 10 proteins are fixed to be 100 μM. The blue, red, and green curves correspond to the concentration of the remaining protein to be 1, 10, and 100 μM, respectively (the blue and red curves overlap). D, The TF coexists with 101 proteins, 100 proteins of which have the same fixed concentration: 100 μM. The blue, red, and green curves correspond to the concentration of the remaining protein to be 1, 10, and 100 μM, respectively (the blue, red, and green curves overlap). The three curves overlap, indicating that changing the concentration of the remaining protein does not affect [4Ca2+–CaM–TF$_1$]. E, $\frac{[4Ca^{2+} - CaM - TF]}{[4Ca^{2+} - CaM - TF]_{ss}}$ for all nine curves shown in (B), (C), and (D), indicating that, for all nine cases, the maximum of $\frac{[4Ca^{2+} - CaM - TF]}{[4Ca^{2+} - CaM - TF]_{ss}}$ reaches at least 9,000-fold. In this graph, 7 out of 9 curves overlap and only three curves are discernible.

Examination of Equation 3 reveals that the existence of a large number of CaM-binding proteins in plant cells can form a buffering system such that the concentration of a CaM-binding TF-specific active signal is insensitive to change in the concentration of another CaM-binding protein. This is because of the two summation terms, $\sum_{j=1}^{n} \frac{P_j[\mathrm{TF}_j]}{K_{j,14}}$ and $\sum_{j=1}^{n} \frac{[\mathrm{TF}_j]}{K_{j,14}}$, in the denominator of Equation 3. Firstly, the existence of any CaM-binding protein, TF_j, always reduces the concentration of the active complex of TF, TF_i. This is because when CaM binds with TF_j, the concentration of CaM available for binding with TF_i will become smaller. In Equation 3, this corresponds to $\sum_{j=1}^{n} \frac{P_j[\mathrm{TF}_j]}{K_{j,14}}$ and $\sum_{j=1}^{n} \frac{[\mathrm{TF}_j]}{K_{j,14}}$ always being larger than $\frac{P_i[\mathrm{TF}_i]}{K_{i,14}}$ and $\frac{[\mathrm{TF}_i]}{K_{i,14}}$, respectively. Secondly, because each of the two terms is the summation of the contribution of all CaM-binding proteins, the TF or protein that contributes a larger value of $\frac{P_j[\mathrm{TF}_j]}{K_{j,14}}$ and $\frac{[\mathrm{TF}_j]}{K_{j,14}}$ is quantitatively more important. Thirdly, as the number of CaM-binding proteins increases, the contribution of each protein to both summation terms becomes less important. When there are only relatively few CaM-binding proteins, changing the concentration of one can change the value of both terms to a relatively large extent. However, if there are many CaM-binding proteins, changing the concentration of one will change the value of both terms to a much lesser extent. For example, we consider that $P_j = 1.0$, $K_{j,14} = 1.0\ \mu\mathrm{M}$, and $[\mathrm{TF}_j] = 100\ \mu\mathrm{M}$ with $j = 1,\ldots n$. When one TF, TF_i, coexists with another TF, TF_j, increasing $[\mathrm{TF}_i]$ from 10 to 100 μM leads to that $\sum_{j=1}^{n} \frac{P_j[\mathrm{TF}_j]}{K_{j,14}}$ increases to 200 from 110, namely an approximate increase of 82% in $\sum_{j=1}^{n} \frac{P_j[\mathrm{TF}_j]}{K_{j,14}}$. However, when one transcription factor, TF_i, coexists with another 100 transcription factors, TF_j, increasing $[\mathrm{TF}_i]$ from 10 μM to 100 μM leads to that $\sum_{j=1}^{n} \frac{P_j[\mathrm{TF}_j]}{K_{j,14}}$ increases to 10,100 from 10,010, namely an approximate increase of 0.9% in $\sum_{j=1}^{n} \frac{P_j[\mathrm{TF}_j]}{K_{j,14}}$.

Thus, existence of a large number of CaM-binding proteins forms a buffering system, in which the concentration of a CaM-binding TF-specific active signal is insensitive to changes in the concentration of another CaM-binding TF or protein. An example of this is shown in Figure 2.

In this example, we assume that $[\mathrm{TF}_1]_t$, the total concentration of a CaM-binding transcription factor, TF_1, is 10 μM. We compare how $[4\mathrm{Ca}^{2+} - \mathrm{CaM} - \mathrm{TF}_1]$, which is the concentration of the active signal of TF_1, depends upon the concentration of a CaM-binding protein when different numbers of other CaM-binding proteins coexist. Figure 2A represents an experimentally measured calcium signature (Whalley et al., 2011). Figure 2B shows that, when the transcription factor, TF_1, competes for CaM binding with one CaM-binding protein, TF_2, changing the total concentration of TF_2, $[\mathrm{TF}_2]_t$, from 1 to 10 μM and 100 μM markedly affects $[4\mathrm{Ca}^{2+} - \mathrm{CaM} - \mathrm{TF}_1]$. Thus, when the calcium signature, as shown in Figure 2A, emerges, although the total concentration of the CaM-binding transcription factor TF_1, $[\mathrm{TF}_1]_t$, remains unchanged (i.e. 10 μM), changing the total concentration of the CaM-binding proteinTF_2, $[\mathrm{TF}_2]_t$, alters the capability of TF_1 for generating an active calcium signal. This is because the concentration of the active signal of TF_1, $[4\mathrm{Ca}^{2+} - \mathrm{CaM} - \mathrm{TF}_1]$, has changed due to the competition between the CaM-binding transcription factor, TF_1, and the CaM-binding protein,TF_2, for binding with CaM. In Figure 2C, the number of CaM-binding proteins TF_jincreases to 11 (i.e. $j = 2,\ldots 12$). Because the number of CaM-binding proteins has increased, changing the total concentration of one CaM-binding protein, $[\mathrm{TF}_2]_t$ (the concentrations of other 10 CaM-binding proteins remain unchanged), from 1 to 10 μM and 100 μM only slightly affects $[4\mathrm{Ca}^{2+} - \mathrm{CaM} - \mathrm{TF}_1]$. Moreover, when the number of CaM-binding proteins TF_j further increases to 101 (i.e. $j = 2,\ldots 102$), the effects of changing the total concentration of one CaM-binding protein, $[\mathrm{TF}_1]_t$, from 1 to 10 μM and 100 μM on $[4\mathrm{Ca}^{2+} - \mathrm{CaM} - \mathrm{TF}_1]$ becomes negligible (Fig. 2D). Thus, when a large number of CaM-binding proteins coexist, a calcium signature, as shown in Figure 2A, can generate a TF-specific active signal, $[4\mathrm{Ca}^{2+} - \mathrm{CaM} - \mathrm{TF}_1]$, to mediate specific changes in gene expression. The concentration of such an active signal is insensitive to changes in the concentration of other CaM-binding proteins. Therefore, the existence of a large number of CaM-binding proteins results in the fidelity of a calcium signature to its TF-specific active signal.

In addition, Figure 2E shows that the concentration of the active calcium signal of TF_1, $[4\mathrm{Ca}^{2+} - \mathrm{CaM} - \mathrm{TF}_1]$, is always amplified regardless of the number of CaM-binding proteins. Therefore, the coexistence of a large number of CaM-binding proteins in plant cells does not affect the intrinsic property of amplifying calcium signatures for Ca^{2+}–CaM–TF interactions. In this way, the nonlinear amplification of calcium signatures, as demonstrated in Figure 2E, allows plant cells to effectively distinguish the kinetics of different calcium signatures to produce specific changes in gene expression, despite the coexistence of a large number of CaM-binding proteins in plant cells.

Specific Gene Expression Responses to Calcium Signatures Require an Appropriate Relationship between the Active Signal Concentration and DNA Binding Affinity

Gene expression is a complex process, which involves both transcription and mRNA degradative processes. Both processes can be regulated in response to signaling. For example, transcriptional processes can be regulated by calcium signals (Reddy et al., 2011; Seybold et al., 2014; Fromm and Finkler, 2015; Tsuda and Somssich, 2015; Zhu, 2016). Moreover, gene expression can form a network, in which the expression of one gene can be regulated by other

genes (Reddy et al., 2011; Seybold et al., 2014; Fromm and Finkler, 2015; Tsuda and Somssich, 2015; Zhu, 2016).

Here we concentrate on elucidating the mechanism for the information flow from calcium signals to a specific gene expression response. To do so, we consider a simple Ca^{2+}-regulated gene expression process: The transcriptional rate is regulated by calcium signals. The principle revealed by this simple example can be applied to more complex gene expression processes, as will be demonstrated in "Case Study 2: Plant Immunity Gene Expression."

Equation 4 describes that the transcription of a gene that is positively regulated by calcium signals:

$$\frac{d[\mathrm{mRNA}]}{dt} = V - k_{\mathrm{decay}}[\mathrm{mRNA}]$$

with

$$V = k_{\mathrm{base}} + \frac{V_{\max}\frac{[4\mathrm{Ca}^{2+} - \mathrm{CaM} - \mathrm{TF}_i]}{k_d}}{1 + \frac{[4\mathrm{Ca}^{2+} - \mathrm{CaM} - \mathrm{TF}_i]}{k_d}} \quad (4)$$

Here, V is the transcription rate; k_{decay} is the decay constant of the mRNA; k_{base} is the base rate of transcription; $V_{\max}$ is the maximal transcription rate regulated by calcium signals; and k_d is the binding affinity between the active complex, $4Ca^{2+}$–CaM–TF_i, and DNA.

As analyzed above, when any calcium signature emerges in an environment of multiple proteins competing for CaM binding, $[Ca^{2+}]$ is amplified into a robust TF-specific active complex for any CaM binding transcription factor, $4Ca^{2+}$–CaM–TF_i. Equation 4 shows that, because $4Ca^{2+}$–CaM–TF_i is always amplified for any calcium signature, the transcription rate, V, will effectively be different for different calcium signatures, leading to a different specific gene expression response in each case. Examination of Equation 4 reveals how the relationship of k_{base}, k_d, and $[4Ca^{2+} - \mathrm{CaM} - \mathrm{TF}_i]$ determines Ca^{2+}-regulated gene expression. If $k_{\mathrm{base}} \gg \frac{V_{\max}\frac{[4\mathrm{Ca}^{2+} - \mathrm{CaM} - \mathrm{TF}_i]}{k_d}}{1 + \frac{[4\mathrm{Ca}^{2+} - \mathrm{CaM} - \mathrm{TF}_i]}{k_d}}$, the base rate of transcription is more important than the rate regulated by the calcium signal. Thus, the effects of a calcium signature on gene expression are negligible under these particular conditions. If $k_d \gg [4Ca^{2+} - \mathrm{CaM} - \mathrm{TF}_i]$, the effects of a calcium signature on gene expression is limited, which is because the term $\frac{V_{\max}\frac{[4\mathrm{Ca}^{2+} - \mathrm{CaM} - \mathrm{TF}_i]}{k_d}}{1 + \frac{[4\mathrm{Ca}^{2+} - \mathrm{CaM} - \mathrm{TF}_i]}{k_d}}$ can become very small. If $k_d \ll [4Ca^{2+} - \mathrm{CaM} - \mathrm{TF}_i]$, the effects of any calcium signature would become approximately a constant $V_{\max}$. Thus, in this case different calcium signatures induce similar transcription rates, leading to similar levels of mRNA. Therefore, for a specific gene expression response to calcium signatures to be generated, $[4Ca^{2+} - \mathrm{CaM} - \mathrm{TF}_i]$ should be not much larger or smaller (e.g. two orders larger or smaller) than k_d. Under this condition, different calcium signatures can be decoded to generate specific gene expression responses. Figure 3 summarizes the design principle that governs the binding mechanism among Ca^{2+}, CaM, and TF, which emerges from two pairs of Ca^{2+}-binding EF-hand domains, a TF-binding domain in CaM, and a CaM-binding domain in the TF, leading to specific gene expression.

In summary, the design principle of Ca^{2+}–CaM–TF interactions includes the following three key aspects for information flow from calcium signals to gene expression: (1) nonlinear amplification of a calcium signal; (2) generation of a Ca^{2+}-induced TF-specific active signal; and (3) (once the binding affinity between the active calcium signal and DNA is appropriate), generation of specific gene expression responses.

Below, we use two examples to demonstrate how calcium signatures generate specific gene expression responses following the design principle revealed herein.

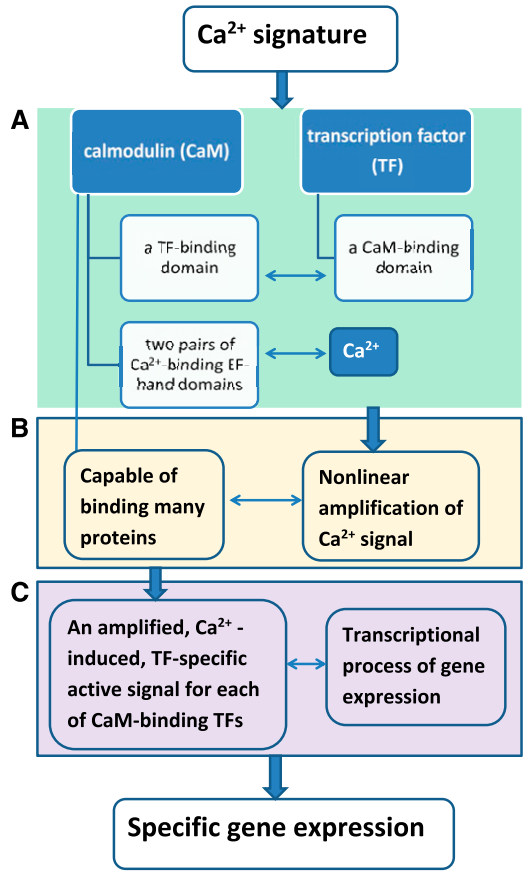

Figure 3. Diagram showing the design principle for transcriptionally decoding calcium signatures to generate specific gene expression. A, The binding mechanism among Ca^{2+}, CaM, and TF, which emerges from two pairs of Ca^{2+}-binding EF-hand domains, and a TF-binding domain in CaM and a CaM-binding domain in TF. B, Nonlinear amplification of Ca^{2+} signal emerges from (A). C, An amplified, Ca^{2+}-induced, TF-specific active signal for each of the CaM-binding TFs emerges from (A) and (B).

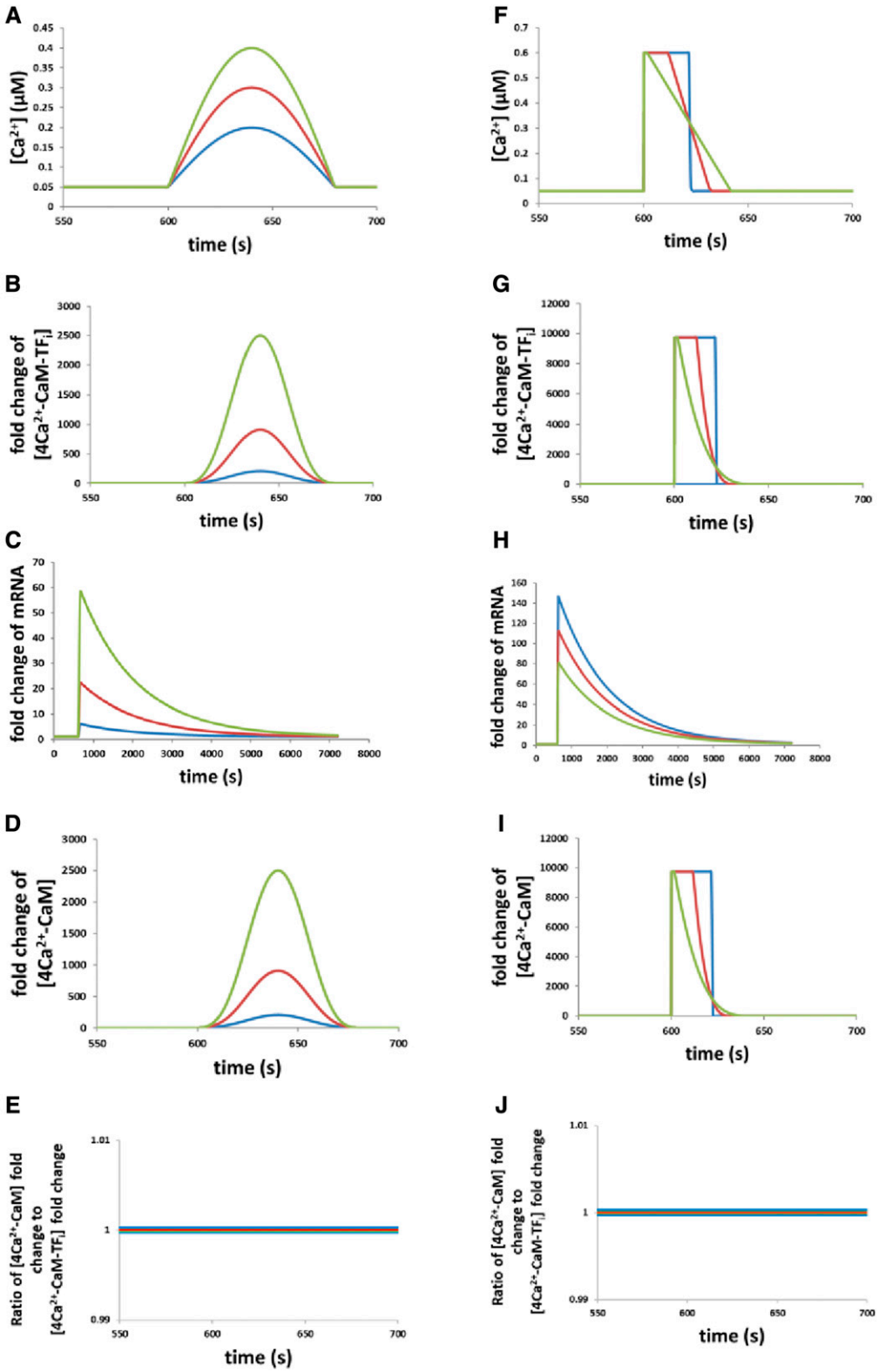

Figure 4. Three similar calcium signatures are decoded to generate specific gene expression responses for a simple Ca^{2+}-regulated gene expression process. A, Three artificial calcium signatures with the same sinusoidal kinetics (the period is fixed to be 80 s, and amplitudes are 0.2, 0.3, and 0.4 μM, respectively; only one period of the sinusoidal kinetics is used). B, $\frac{[4Ca^{2+} - CaM - TF]}{[4Ca^{2+} - CaM - TF]_{ss}}$ calculated using the three calcium signatures in (A) as the input of Equation 3. C, Fold change of mRNA corresponding to the three calcium signatures in (A). D, $\frac{[4Ca^{2+} - CaM]}{[4Ca^{2+} - CaM]_{ss}}$ calculated using the three calcium signatures in (A) as the input of

Case Study 1: A Simple Ca^{2+}-Regulated Gene Expression System

To test how the design principle summarized in Figure 3 governs the decoding of different calcium signatures to generate specific gene expression responses, we first studied a simple theoretical gene expression system described by Equation 4 using artificial calcium signatures. An advantage of artificial calcium signatures is that the parameters of different calcium signatures can be compared with each other so that effects of those parameters of calcium signatures on gene expression can be examined. In addition, investigating both artificial calcium signatures in this case study and examining experimentally measured calcium signatures in Case Study 2 below allows us to show that the design principle revealed in this research is generic for any calcium signature.

Figure 4A shows three calcium signatures with the same type of kinetics. All three calcium signatures take a sinusoidal form with the same period, but their amplitudes are different. For simplicity, we study one period of these sinusoidal calcium signatures only. Figure 4B shows that a relatively modest change in the amplitude of these three calcium signatures (0.2 to 0.4 μM) is amplified into large fold differences in the concentration of the active signal, $[4Ca^{2+} - CaM - TF_i]$. Subsequently, this large difference in the concentrations of the three active signals leads to different fold changes of mRNA concentration, as shown in Figure 4C. We emphasize that the large difference (from approximately maximum 6-fold to approximately maximum 58-fold) in mRNA concentrations in Figure 4C stems entirely from the relatively modest difference in the amplitude of the three calcium signatures (0.2 to 0.4 μM), as the kinetics of the three calcium signatures is the same. Derivation of Equation 2 in the Supplemental Text reveals that the term $\left(\frac{[Ca^{2+}]}{[Ca^{2+}]_{ss}}\right)^4$ emerges from two pairs of Ca^{2+}-binding EF-hand domains and a TF-binding domain in the CaM structure. Therefore, the ability of CaM to bind four Ca^{2+} and one TF molecule results in the amplification of calcium signal. Figure 4D further shows that the fold change of $[4Ca^{2+} - CaM]$ is approximately the same as that of $[4Ca^{2+} - CaM - TF_i]$, as shown in Figure 4B, and this is also confirmed in Figure 4E. Therefore, Figure 4, B, D, and E together reveal that the amplification of the calcium signatures, shown in Figure 4A, is originated from two pairs of Ca^{2+}-binding EF-hand domains in the CaM structure and that it is further relayed to the binding between $4Ca^{2+}$–CaM complex and TF.

Figure 4F shows three calcium signatures with the same average calcium concentration (0.2 μM). The difference between the three calcium signatures is their kinetics. Figure 4G shows that these relatively slight differences in the kinetics of these three calcium signatures is amplified into the kinetics of the active signal, $[4Ca^{2+} - CaM - TF_i]$. Subsequently, Figure 4H shows that the difference in the kinetics of the three active signals leads to different fold changes of mRNA concentration. We emphasize that the difference (from approximately maximum 80-fold to approximately maximum 148-fold) in the fold change of mRNA concentrations in Figure 4H stems solely from the difference in the kinetics of the three calcium signatures, as the average calcium concentration is the same for the three calcium signatures. Following the analysis represented by Figure 4, D, E, G, I, and J, together reveal that the amplification of the calcium signatures shown in Figure 4F also originates from two pairs of Ca^{2+}-binding EF-hand domains in the CaM structure and that it is further relayed to the binding between $4Ca^{2+}$–CaM complex and TF.

Therefore, Figure 4 shows that different calcium signatures, displaying only modest differences, can generate very different specific gene expression responses following the design principle.

Another aspect of the design principle is that when a large number of CaM-binding proteins coexist, a calcium signature is able to generate a specific gene expression response, which is not affected by the concentrations of another CaM-binding protein. The numerical analysis shown in Figure 5 confirms that, when a large number of CaM-binding proteins coexist, the gene expression response of the simple system remains the same even if the concentration of a CaM-binding protein has changed from 0.01 to 10,000 μM.

When the calcium signature shown in Figure 5A emerges and if one protein and one TF compete for binding with CaM simultaneously, changing the protein concentration affects the TF-specific gene expression, resulting in different fold changes of mRNA (Fig. 5B). However, when a large number of CaM-binding proteins (here 101 proteins) and one TF compete for the binding of CaM, changing the concentration

Figure 4. (*Continued.*)

Equation 3. E, The ratio of $\frac{[4Ca^{2+} - CaM]}{[4Ca^{2+} - CaM]_{ss}}$ to $\frac{[4Ca^{2+} - CaM - TF]}{[4Ca^{2+} - CaM - TF]_{ss}}$. This ratio is always equal to 1, indicating that $\frac{[4Ca^{2+} - CaM]}{[4Ca^{2+} - CaM]_{ss}}$ is always the same as $\frac{[4Ca^{2+} - CaM - TF]}{[4Ca^{2+} - CaM - TF]_{ss}}$. F, Three artificial calcium signatures with the same average calcium concentration (the average of $[Ca^{2+}]$ is 0.2 μM for each of the three curves). G, $\frac{[4Ca^{2+} - CaM - TF]}{[4Ca^{2+} - CaM - TF]_{ss}}$ calculated using the three calcium signatures in (F) as the input of Equation 3. H, Fold change of mRNA corresponding to the three calcium signatures in (F). I, $\frac{[4Ca^{2+} - CaM]}{[4Ca^{2+} - CaM]_{ss}}$ calculated using the three calcium signatures in (F) as the input of Equation 3. J, The ratio of $\frac{[4Ca^{2+} - CaM]}{[4Ca^{2+} - CaM]_{ss}}$ to $\frac{[4Ca^{2+} - CaM - TF]}{[4Ca^{2+} - CaM - TF]_{ss}}$. This ratio is always equal to 1, indicating $\frac{[4Ca^{2+} - CaM]}{[4Ca^{2+} - CaM]_{ss}}$ is always the same as $\frac{[4Ca^{2+} - CaM - TF]}{[4Ca^{2+} - CaM - TF]_{ss}}$.

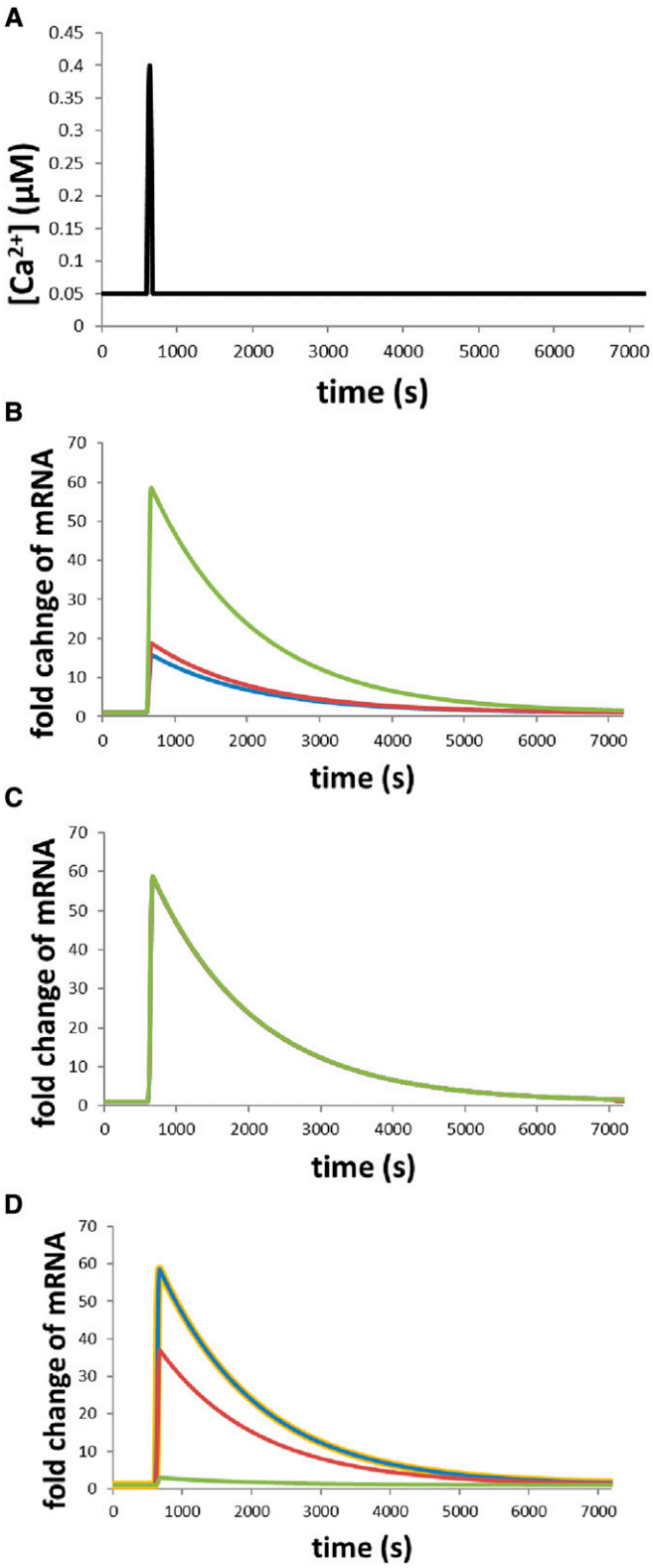

Figure 5. Effects of the number of CaM-binding proteins or the binding rates on specific gene expression responses for a simple Ca^{2+}-regulated gene expression process. A, An artificial calcium signature. B, Effects of the number of CaM-binding proteins on specific gene expression responses. The TF coexists with one protein. Green, red, and blue curve corresponds to the concentration of the protein to be 1, 10, and 100 μM, respectively. C, Effects of the number of CaM-binding proteins on specific gene expression responses. The TF coexists with 101 proteins, 100 proteins of which have the same fixed concentration: 100 μM. The green, red, and blue curves correspond to the concentration of the remaining protein to be 1, 10, and 100 μM, respectively. The three curves overlap, indicating that changing the concentration of the remaining protein does not affect fold change of mRNA. D, Effects of the binding rates on specific gene expression responses. The wide orange curve is calculated using Equation 3. The blue curve is calculated using differential equations with all experimentally determined on- and off-binding rates (Shifman et al., 2006; Pepke et al., 2010). The wide orange curve and the blue curve overlap, indicating a quasi-equilibrium state has established. The red and green curves correspond to the on- and off-binding rates, which are reduced by 100-fold and 1.0e4-fold, respectively.

of one CaM-binding protein out of 101 (i.e. the concentration of the remaining 100 CaM-binding proteins remains unchanged) does not affect the TF-specific gene expression, resulting in no different fold changes of mRNA (Fig. 5C). Therefore, when many proteins compete for CaM binding, specific gene expression responses to calcium signatures are robust, and TF-specific. This is because the concentration of a CaM-binding TF-specific active signal is insensitive to changes in another CaM-binding TF or protein concentration when a large number of CaM-binding proteins coexist, as analyzed in Figure 2.

Figures 4 and 5 together explain how the interaction among Ca^{2+}, CaM, and the CaM-binding TFs induces specific gene expression responses in the simple Ca^{2+}-regulated gene expression process described by Equation 4. Therefore, this demonstrates that the design principle, shown in Figure 3, establishes the link between calcium signatures and specific gene expression responses induced by the signatures.

The dynamics for the interactions between Ca^{2+}, CaM, and CaM-binding proteins can be generally examined using differential equations (Pepke et al., 2010; Liu et al., 2015; Lenzoni et al., 2018). If a quasi-equilibrium state for the interactions of Ca^{2+}, CaM, and CaM-binding proteins has been established, all differential equations describing the interactions among Ca^{2+}, CaM, and CaM-binding proteins become zero and Equations 1 to 3 *c*an be derived. Figure 5D further examines the validity and effects of the quasi-equilibrium assumption for deriving Equations 1 to 3. Figure 5D shows that, for experimentally measured parameters of Ca^{2+}-CaM binding constants (Shifman et al., 2006; Pepke et al., 2010), the gene expression response curve computed without the quasi-equilibrium assumption for the interactions of Ca^{2+}, CaM, and CaM-binding proteins (i.e. differential equations) overlaps with the gene expression response curve computed with the quasi-equilibrium assumption (i.e. Equation 3), indicating that a quasi-equilibrium state of Ca^{2+}–CaM–TF interaction in plant cells has been established.

Although the quasi-equilibrium state assumption is valid for experimentally measured parameters of Ca^{2+}–CaM binding constants, reducing those parameters may make the assumption invalid. We further test how validity of the assumption affects gene expression responses. When all on- and off-rate constants for Ca^{2+}–CaM interactions are simultaneously reduced by the same fold from their experimentally measured values (Shifman et al., 2006; Pepke et al., 2010), the equilibrium constants for all Ca^{2+}–CaM binding processes remain the same as the experimental values. This is because an equilibrium constant is the ratio between the off-rate constant and the on-rate constant. However, if all on- and off-rate constants are simultaneously reduced, the quasi-equilibrium assumption may become invalid due to slow binding rates. Figure 5D shows that when all on- and off-rate constants for Ca^{2+}–CaM interactions are simultaneously reduced by 100-fold, the quasi-equilibrium assumption becomes invalid. Once this happens, the calcium signature, as shown in Figure 5A, is less capable of inducing a gene expression response. In addition, Figure 5D also shows that very small Ca^{2+}–CaM on- and off-rate constants (i.e. they are reduced by 1.0e4-fold from their experimental values) render gene expression response to calcium signatures impossible. This implies that establishing a quasi-equilibrium state is favorable for a calcium signature to induce gene expression responses.

Another important aspect of the design principle, as described in Figure 3, is that specific gene expression responses to calcium signatures require an appropriate relationship between the active signal concentration, $[4Ca^{2+} - CaM - TF_i]$, and DNA binding affinity. The dissociation equilibrium constant (i.e. the binding affinity) for the binding of the Ca^{2+}–CaM complex to a TF is an important parameter. Changing the value of the dissociation equilibrium constant changes $[4Ca^{2+} - CaM - TF_i]$, and therefore affects the relationship between $[4Ca^{2+} - CaM - TF_i]$ and DNA binding affinity. Supplemental Figure S1 shows the effects of the dissociation equilibrium constant for the binding of the Ca^{2+}–CaM complex to a transcription factor, K_{14}, on gene expression regulated by the TF. Supplemental Figure S1A shows an artificial calcium signature. Supplemental Figure S1B shows that decreasing the value of K_{14} increases the steady-state value of $[4Ca^{2+} - CaM - TF_i]$. Similarly, Supplemental Figure S1C shows that decreasing the value of K_{14} increases the value of $[4Ca^{2+} - CaM - TF_i]$ responding to the calcium signature. Supplemental Figure S1D shows that, for the three different values of K_{14}, the calcium signature is always amplified. Supplemental Figure S1, E to G, shows that, although decreasing the value of K_{14} increases both the steady-state mRNA concentration and the mRNA concentration responding to the calcium signature, three different values of K_{14} lead to three different responses of mRNA concentration to the calcium signature. Therefore, different TFs with different values of K_{14} can generate different responses of mRNA concentration to a calcium signature. This indicates that the dissociation equilibrium constant for the binding of the Ca^{2+}–CaM complex to a transcription factor, K_{14}, is an important parameter for specific gene expression responses to a calcium signature. Similarly, analysis in Supplemental Figure S2 for a different artificial calcium signature also supports the above conclusion.

In summary, this example shows that, for the simple gene expression system described by Equation 4, different calcium signatures can be decoded to generate specific gene expression responses following the design principle, as described in Figure 3.

Case Study 2: Plant Immunity Gene Expression

The CaM-binding TFs CAMTA3 (AtSR1) and CBP60g regulate the expression of two important plant immunity genes: *EDS1* and *ICS1* (Zhang et al., 2010, 2014). Recently, we developed a dynamic model to determine how expression of both *EDS1* and *ICS1* is regulated by different calcium signatures and analyzed the model using computer simulation of differential equations (Lenzoni et al., 2018). It was demonstrated that the model was able to predict the expression of both *EDS1* and *ICS1* (Lenzoni et al., 2018). Here we use this system as an example to study how the expression response of both *EDS1* and *ICS1* to calcium signatures is generated following the design principle, as shown in Figure 3.

Figure 6, A and B, shows two empirically derived calcium signatures induced by two calcium agonists: mastoparan and extracellular calcium (Lenzoni et al., 2018). The model developed for studying how expression of both *EDS1* and *ICS1* (Lenzoni et al., 2018) is regulated by different calcium signatures employed experimentally measured parameters for both Ca^{2+}–CaM binding (Shifman et al., 2006; Pepke et al., 2010) and CaM-CAMTA3 binding (Bouché et al., 2002; Finkler et al., 2007). Figure 6, C and F, shows that, for these experimentally measured on- and off-rate constants for Ca^{2+}–CaM interactions, the curve calculated using differential equations overlaps with the curve calculated using Equation 3 for both $[4Ca^{2+} - CaM - CAMTA3]$ and $[4Ca^{2+} - CaM - CBP60g]$, indicating that the quasi-equilibrium assumption for interactions of Ca^{2+}–CaM–CAMTA3 and Ca^{2+}–CaM–CBP60g, as well as the interactions of Ca^{2+}, CaM, and 100 other CaM-binding proteins are valid. Thus, the two active signals in Figure 6, C and F, $4Ca^{2+}$–CaM–CAMTA3 and $4Ca^{2+}$–CaM–CBP60g, are differentially induced by the two calcium signatures (Fig. 6, A and B). Moreover, Supplemental Figure S3, C and F, shows that the two active signals are effectively and differentially amplified.

However, when both on- and off-rate constants for Ca^{2+}–CaM interactions are reduced by 1.0e5-fold from their experimental values, the quasi-equilibrium assumption for deriving Equation 3 becomes invalid, as evidenced by the differences between the curve

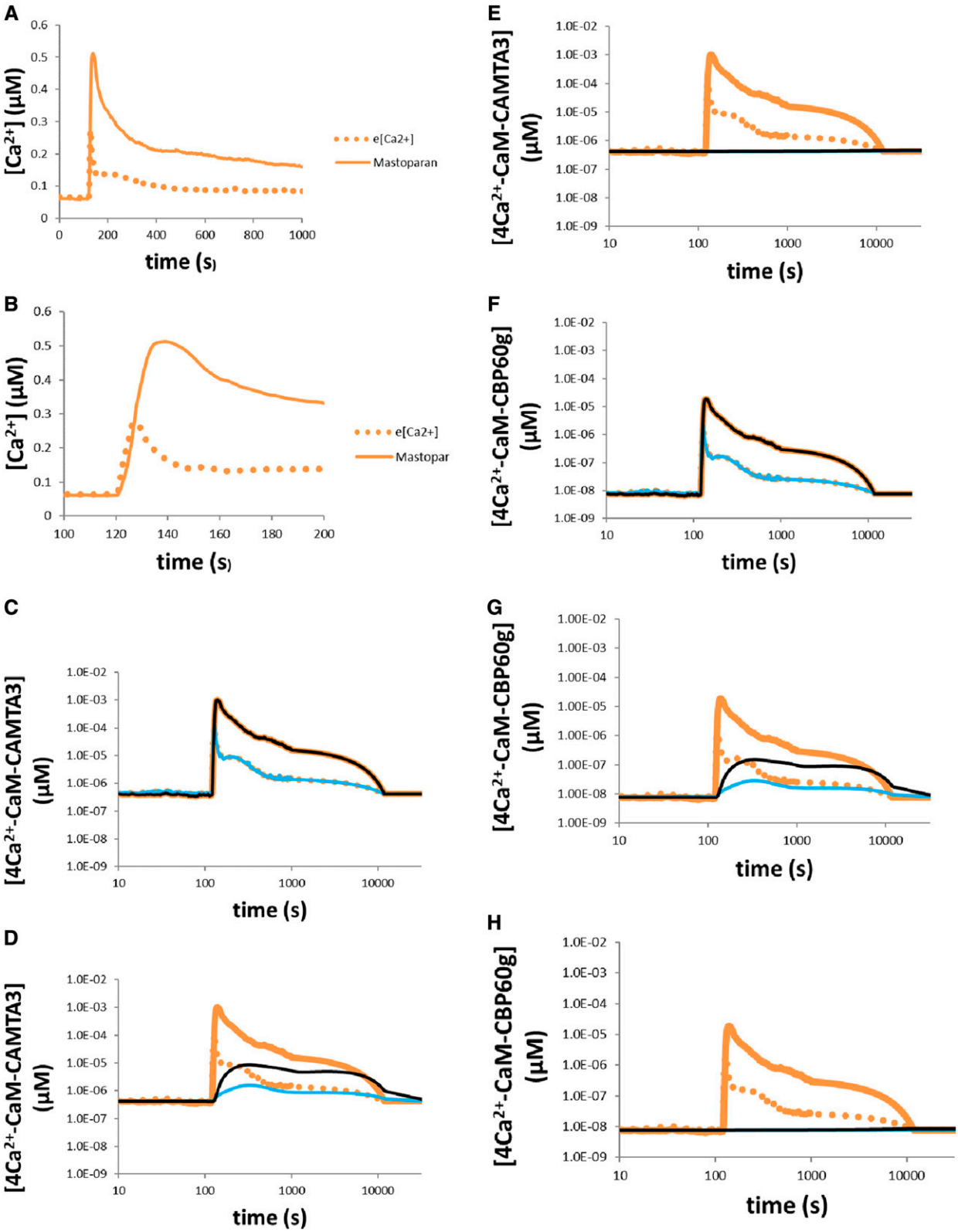

Figure 6. Responses of two active signals, $4Ca^{2}$–CaM–CAMTA3 and $4Ca^{2+}$–CaM–CBP60g, to two experimentally measured calcium signatures. A. Two empirical calcium signatures induced by two calcium agonists: mastoparan and extracellular calcium (Lenzoni et al., 2018). B, Enlargement of (A), showing the details of the two calcium signatures. C, Response of $4Ca^{2+}$–CaM–CAMTA3 to the two calcium signatures. The wide solid orange curve and wide dashed orange curve are calculated

calculated using differential equations and the curve calculated using Equation 3 (Fig. 6, D and G). Moreover, the two active signals in Figure 6, D and G, $4Ca^{2+}$–CaM–CAMTA3 and $4Ca^{2+}$–CaM–CBP60g, are both less effectively amplified (Supplemental Fig. S3, D and G) than in Fig. 6, C and F, indicating that a valid quasi-equilibrium assumption makes the amplification of both active signals more favorable. In addition, when the on- and off-rate constants are reduced by 1.0e8-fold, the two active signals, $4Ca^{2+}$–CaM–CAMTA3 and $4Ca^{2+}$–CaM–CBP60g, cannot respond to either of the two calcium signatures (Fig. 6, A and B), as evidenced by the overlapping of the two flat curves corresponding to the two calcium signatures in Figure 6, E and H. Furthermore, neither of the two active signals in Figure 6, E and H, can be amplified anymore under these conditions (Supplemental Fig. S3, E and H), indicating that very small Ca^{2+}–CaM on- and off-rate constants render amplification of calcium signals impossible.

CAMTA3 and CBP60g are the TFs that regulate the expression of *EDS1* and *ICS1*, respectively (Zhang et al., 2010, 2014). These correspond to the two active signals shown in Figure 6, C and F, the two calcium signatures inducing different mRNA levels for both *EDS1* and *ICS1* genes (Fig. 7, A and D), leading to specific gene expression responses for both genes. Moreover, because the curve calculated using differential equations overlaps with the curve calculated using Equation 3 for the fold change of mRNA of both *EDS1* and *ICS1* (Fig. 7, A and D), gene expression responses of both *EDS1*and *ICS1* to the two calcium signatures clearly follow the design principle (Fig. 3; Eqs. 1–3).

When the on- and off-rate constants for Ca^{2+}–CaM interactions are reduced by 1.0e5-fold, Figure 7, B and E, show that less effective amplification of both active signals, $4Ca^{2+}$–CaM–CAMTA3 and $4Ca^{2+}$–CaM–CBP60g (Fig. 6, D and G; Supplemental Fig. S3, D and G), markedly affects the mRNA level of both *ICS1* and *EDS1*. Furthermore, when the on- and off-rate constants for Ca^{2+}–CaM interactions are reduced by 1.0e8-fold, no amplification of either of the two active signals, $4Ca^{2+}$–CaM–CAMTA3 and $4Ca^{2+}$–CaM–CBP60g, occurs (Fig. 6, E and H; Supplemental Fig. S3, E and H), leading to no change in expression of either *EDS1* or *ICS1*. This is evidenced by the overlapping of the two flat curves corresponding to the two calcium signatures in Figure 7, C and F, showing no change in gene expression response to either signature.

In conclusion, for experimentally measured on- and off-rate constants (Shifman et al., 2006; Pepke et al., 2010), the two calcium signatures (Fig. 6, A and B) are decoded following the design principle to generate specific expression of both *EDS1* and *ICS1* (Fig. 7, A and D). If the on- and off-rate constants for Ca^{2+}–CaM interactions are largely reduced (e.g. 1.0e8-fold), specific gene expression responses to the two calcium signatures become impossible (Fig. 7, C and F). Therefore, the actual values of on- and off-rate constants for Ca^{2+}–CaM interactions, as experimentally measured in the literature (Shifman et al., 2006; Pepke et al., 2010), ensure that plant immunity gene expression responses of both *EDS1* and *ICS1* follow the design principle to decode the two calcium signatures induced by two calcium agonists: mastoparan and extracellular calcium (Fig. 6, A and B).

DISCUSSION

Most stimuli lead to a transient elevation in cellular calcium concentration in plant cells. Importantly, different stimuli produce calcium elevations with different characteristics: a unique calcium signature. These calcium signatures are decoded to generate specific responses (Edel et al., 2017; Yuan et al., 2017; Bender et al., 2018; Kudla et al., 2018). An intriguing question: How can one messenger (Ca^{2+}) be decoded by so many decoders (TFs and proteins) in plant cells (Edel et al., 2017)?

Design principles are the underlying properties of network structures that have evolved to endow the network functions. This work reveals the design principle for decoding calcium signals to generate specific gene expression response in plant cells via transcription. The design principle links the structural characteristics of CaM and TF with the capability of decoding calcium signatures in plant cells, and it therefore reveals how the mechanism of Ca^{2+}, CaM, and TF interactions leads to specific gene expression. It includes the following three important aspects: Firstly, the binding mechanism between Ca^{2+}, CaM, and TF, which emerges from two pairs of Ca^{2+}-binding EF-hand domains and a TF-binding domain in the CaM structure, possesses an intrinsic property of amplifying calcium

Figure 6. (*Continued.*)
using the two calcium signatures as the input of Equation 3, respectively. Experimentally measured parameters are used. The black and blue curves are calculated using the two calcium signatures as the input of differential equations, respectively. The wide orange curve overlaps with the black curve. The wide dashed orange curve overlaps with the blue curve. These results indicate a quasi-equilibrium state is established. D, Same as (C), but both on- and off-rate constants for Ca^{2+}–CaM interactions are reduced by 1.0e5-fold from their experimental values. E, Same as (C), but both on- and off-rate constants for Ca^{2+}-CaM interactions are reduced by 1.0e8-fold from their experimental values. The black and blue curves are flat and they also overlap, indicating that neither calcium signature can induce changes in $\left[4Ca^{2+} - CaM - CAMTA3\right]$. F, Same as (C), but it is the response of $4Ca^{2+}$–CaM–CBP60g to the two calcium signatures. G, Same as (F), but both on- and off-rate constants for Ca^{2+}–CaM interactions are reduced by 1.0e5-fold from their experimental values. H, Same as (F), but both on- and off-rate constants for Ca^{2+}–CaM interactions are reduced by 1.0e8-fold from their experimental values. The black and blue curves are flat and they also overlap, indicating that neither calcium signature can induce changes in $[4Ca^{2+} - CaM - CBP60g]$.

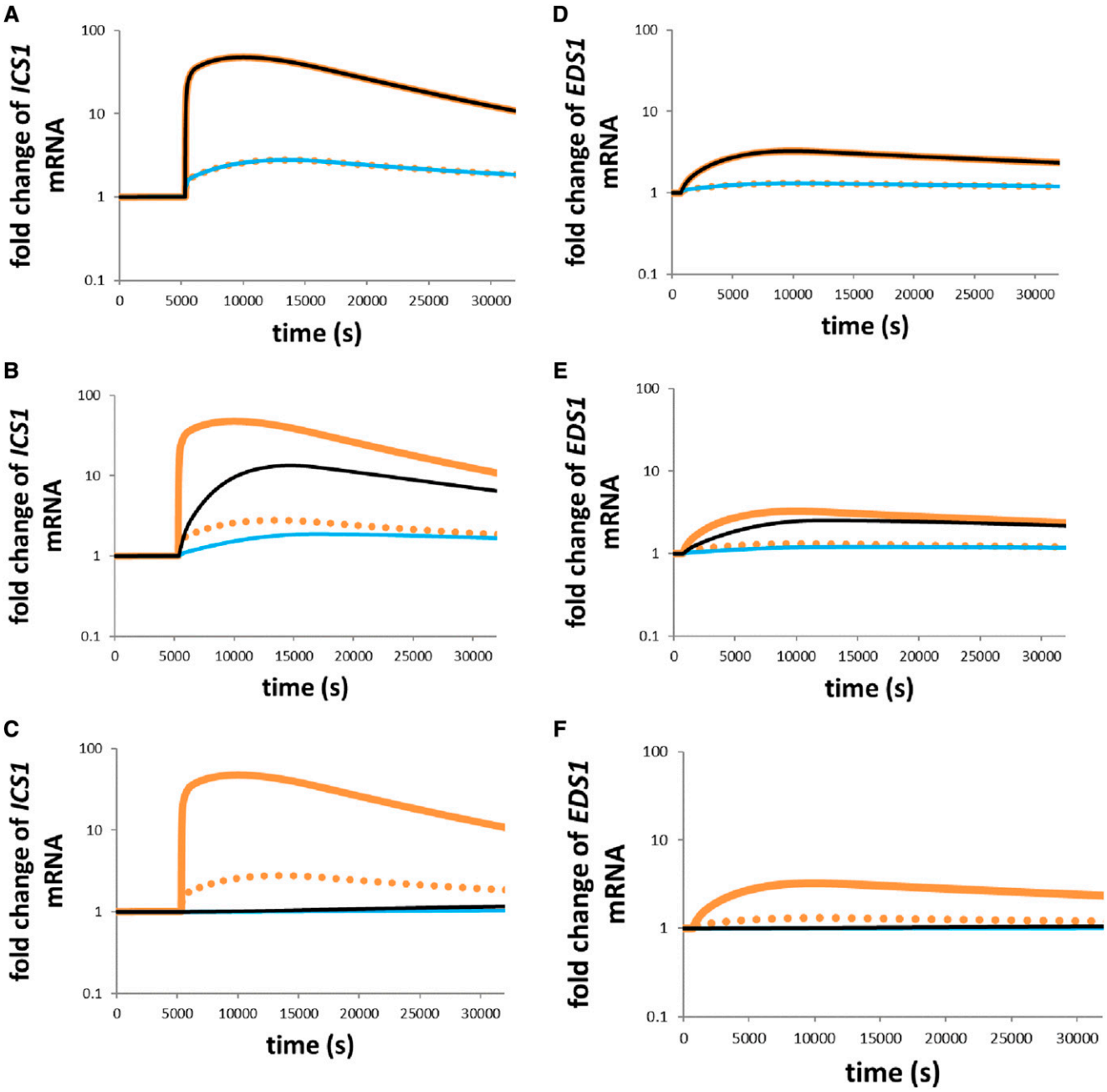

Figure 7. Fold change of both *EDS1* and *ICS1* mRNA responding to two experimentally measured calcium signatures. A, Same as Figure 6, C and F, but it is the fold change of *ICS1* mRNA. B, Same as Figure 6, D and G, but it is the fold change of *ICS1* mRNA. C, Same as Figure 6, E and H, but it is the fold change of *ICS1* mRNA. D, Same as Figure 6, C and F, but it is the fold change of *EDS1* mRNA. E, Same as Figure 6, D and G, but it is the fold change of *EDS1* mRNA. F, Same as Figure 6, E and H, but it is the fold change of *EDS1* mRNA.

signals in the format of $\left(\frac{[Ca^{2+}]}{[Ca^{2+}]_{ss}}\right)^4$ being multiplied by a factor that is relatively less important. We derived the equations for describing the amplification of calcium signals (Eqs. 1 and 2) and mathematically proved that calcium signals are always amplified (Supplemental Text). Because any calcium signature is always amplified, small differences in the kinetics or parameters of calcium signatures can be read out to generate relatively much larger specific gene expression responses (Figs. 4 and 5). Secondly, the existence of a large number of CaM-binding TFs or proteins in plant cells (Reddy et al., 2011; Poovaiah et al., 2013; Virdi et al., 2015; Edel et al., 2017; Yuan et al., 2017; Bender et al., 2018; Kudla et al., 2018) can form a buffering system such that the concentration of a CaM-binding TF-specific active

signal is insensitive to changes in the concentration of another CaM-binding TF or protein (Fig. 2D). Thus, although many proteins compete for the binding of CaM, Ca^{2+}-induced TF-specific gene expression will not in fact be affected by the concentration of another CaM-binding TF or protein (Fig. 5C) in plant cells. Although a TF-specific gene expression event must be controlled by the concentration of this TF, it would not be advantageous if it can also be altered by changes in the concentrations of other proteins. This is a clear example of inbuilt robustness of the network endowed by the design principle. Our results also show that when a CaM-binding TF competes for CaM binding with one or a few CaM-binding TFs and proteins, gene expression regulated by a CaM-binding TF will be interfered with by another CaM-binding TF or protein (Fig. 5C). Thus, competition of CaM-binding TFs or proteins for CaM binding may have a role in the relationship between calcium signals and gene expression response if a small number of CaM-binding TFs or proteins exist in plant cells. Interestingly, for postsynaptic cells, a model in which six proteins compete for CaM binding, competition plays a role in setting the frequency-dependence of Ca^{2+}-dependent proteins (Romano et al., 2017), and therefore it was suggested that competitive tuning could be an important dynamic process underlying synaptic plasticity. Therefore, both our work and the results in the literature (Romano et al., 2017) suggest that competition of a small number of CaM-binding proteins will cause the response of one CaM-binding protein to calcium signals to be affected by other CaM-binding proteins. Thirdly, an appropriate relationship between a Ca^{2+}-induced TF-specific active signal concentration and its DNA binding affinity is important for a Ca^{2+}-induced TF-specific gene expression response. For a Ca^{2+}-induced TF-specific active signal to generate gene expression responses, its concentration needs to be similar to the binding affinity between the signal and DNA. In general, for any binding to perform biological functions, the affinity between a ligand and its binding partner should not be very different from the concentration of the ligand (e.g. the differences not larger than two orders; Kuriyan et al., 2013). Our analysis reveals this aspect is also applicable to Ca^{2+}-induced gene expression systems.

We used two examples to show how gene expression follows the design principle to decode different calcium signatures. Gene expression is generally regulated in a complex way (Karlebach and Shamir, 2008). The simplest gene expression process includes: (1) gene transcription is activated or suppressed by a TF; and (2) the mRNA decays.

Our first example tested how a simple gene expression system decodes different calcium signatures. We found that different kinetics or different parameters (here testing amplitudes of a sinusoidal calcium signature) could be decoded following the design principle. Therefore, this example demonstrated that different calcium signatures, even if their differences are modest (Fig. 4, A and F), can generate specific gene expression responses (Fig. 4, C and H) following the design principle. Experimentally any, even a modest, calcium signature (e.g. in response to ozone (Clayton et al., 1999) is able to induce gene expression. Therefore, our results, shown in Figures 4 and 5, imply that the design principle is a general principle for governing the decoding of calcium signatures in simple gene expression systems, in which transcription rates are regulated by calcium signals.

The second example showed that expression of two plant immunity genes (*EDS1* and *ICS1*) follows the design principle to decode two empirical calcium signatures induced by two calcium agonists (mastoparan and extracellular calcium). Calcium signals regulate the expression of *EDS1* and *ICS1* at two levels. First, CAMTA3 and CBP60g are well-characterized Ca^{2+}/CaM-regulated TFs and both have a CaM-binding domain (Finkler et al., 2007; Galon et al., 2008; Kim et al., 2009; Wang et al., 2009; Zhang et al., 2010; Reddy et al., 2011; Wang et al., 2011; Bickerton and Pittman, 2012; Poovaiah et al., 2013). Thus, calcium signals regulate the activities of both CAMTA3 and CBP60g. Second, expression of *EDS1* and *ICS1* forms a regulatory network (Zhang et al., 2014; Lenzoni et al., 2018) and their expression is regulated by each other via this network (Zhang et al., 2014; Lenzoni et al., 2018). Despite this complexity in regulating the expression of *EDS1* and *ICS1*, the design principle still governs the expression of both *EDS1* and *ICS1*. Thus, our results, shown in Figures 6 and 7, imply that the design principle is a general principle for governing the decoding of calcium signature in complex gene expression systems, in which multiple TFs are regulated by calcium signals and gene expression itself forms a regulatory network.

The design principle, as described in Figure 3 and summarized above, is generic for elucidating the decoding of calcium signals that generate specific gene expression responses via transcription. Therefore, it can be integrated with a wide range of experimental analysis. For example, we have shown how to study gene expression for both simple and complex systems that are regulated by any calcium signatures (Figs. 4–7). Arabidopsis genes responding to simultaneous biotic and abiotic stresses have been experimentally identified (Atkinson et al., 2013). Following the analysis shown in Figures 6 and 7, any genes that are regulated by calcium signals under both biotic and abiotic conditions could be theoretically investigated based on the experimental measurements of gene expression corresponding to the relevant calcium signatures. In addition, the role of CaM binding to CAMTA3 in regulating immunity genes was experimentally investigated (Kim et al., 2017). The design principle could be used to quantitatively analyze this role for different binding domains within CAMTA3. It should be noted that this requires experimental inputs to provide parameters. For example, the binding K_D of CaM to CAMTA3 in the presence of Ca^{2+} had been experimentally measured (Bouché et al., 2002; Finkler et al., 2007). Therefore, it is important that future experiments measure such

parameters for the binding between CaM and other (than CAMTA3) CaM-binding proteins. CaM and other calcium-binding proteins have the potential to regulate and modify calcium signatures themselves. We could address this important aspect of calcium signaling in the future. Some genes regulated by calcium signatures encode proteins with roles in transporting/binding calcium in plant cells (Kudla et al., 2010; Yip Delormel and Boudsocq, 2019). To further study the effects of gene expression on the generation of calcium signatures, the design principle established in this work could in the future be combined with the processes for generation of calcium signature (Medvedev, 2018). This may be important in understanding alterations in calcium signatures as a result of acclimation to stress, and due to interaction between different stresses. For example, the design principle developed in this work can be used to study the effects of the concentrations of CaM and transcriptions on the mRNA levels of gene expression, which can be linked with the processes of calcium transport to quantitatively examine the effects of mRNA levels on generation of calcium signature in the future. To further validate the design principle we present here, the plant immunity system would be a good model. Future experiments could involve complementation of *camta3* and *cbp60g* mutants with *CAMTA3* and *CBP60g* in which the protein coding regions have been modified to alter binding constants to DNA and CaM. The effect of these altered affinities could be predicted using our mathematical model, and tested empirically in the complemented lines by measuring *ICS1*/*EDS1* gene expression in response to applied calcium signatures.

Calcium signals are the lead currency of plant information processing (Dodd et al., 2010; Kudla et al., 2010), and they regulate many different responses in plant cells. However, little is known about the underlying principle for how information flows from calcium signals to specific gene expression responses in plant cells. This work reveals the underlying principles for linking the structure of CaM and TF molecules with calcium-regulated gene expression response through Ca^{2+}–CaM–TF binding mechanism and the emerging property of calcium signal amplification. The design principle indicates that the existing interaction network of Ca^{2+}, CaM, and proteins, which may have been evolutionarily tuned (Edel et al., 2017), effectively navigates calcium signatures to generate specific gene expression responses in plant cells. Experimental data have shown multiple levels of complexities in decoding calcium signals in plant cells (Edel et al., 2017; Yuan et al., 2017; Bender et al., 2018; Kudla et al., 2018). Plants cells possess four main types of Ca^{2+} sensor proteins to relay or decode Ca^{2+} signaling: CaM, CaM-like proteins, calcineurin B-like proteins, and Ca^{2+}-dependent protein kinases (Yuan et al., 2017). These proteins relay or decode calcium signals at both the transcriptional and post-translational levels (Yuan et al., 2017). This work has focused on the interactions among Ca^{2+}, CaM, and TFs at transcriptional level and revealed that transcriptional decoding of calcium signals follows a general design principle. Other Ca^{2+} sensor proteins can have different numbers of Ca^{2+}-binding sites or possess complex molecular structures. For example, CaM-like proteins may have one to six EF-hands and one to four Ca^{2+}-binding sites (La Verde et al., 2018). A Ca^{2+}/CaM-dependent protein kinase possesses three additional Ca^{2+}-binding sites in addition to its CaM-binding site (Miller et al., 2013). Our methodology for unraveling the design principle for transcriptional decoding of calcium signals may be further developed to study the underlying general principle for other Ca^{2+}-regulated signaling systems in the future.

MATERIALS AND METHODS

Ca^{2+}–CaM–Protein Interactions

The interaction among Ca^{2+}, CaM, and any protein can form different binding complexes. CaM has two pairs of Ca^{2+}-binding EF-hand domains located at the N- and C terminus, respectively (Finn and Forsén, 1995; Valeyev et al., 2008). Thus, for a protein with one CaM-binding site, 18 different binding complexes can form via 33 elementary binding processes. A detailed description of these interactions was presented in detail by Liu et al. (2015) and Lenzoni et al. (2018), and the 33 elementary binding processes are included in Supplemental Table S1. Experimentally measured parameters for the interactions between Ca^{2+} and CaM are included in Supplemental Table S2.

Modeling Expression of Plant Immunity Genes

The model used to examine expression of plant immunity genes (*ICS1* and *EDS1*) was described in detail in Lenzoni et al. (2018). The differential equations and parameters of the model were included in Lenzoni et al. (2018). This work uses this model to study how expression of both *ICS1* and *EDS1* decodes calcium signatures following the design principle.

Numerical Method

All computational results are generated using the simulator Berkeley Madonna (www.berkeleymadonna.com). For differential equations, Rosenbrock (Stiff) method is used with a tolerance of 1.0e-5. Much smaller tolerances (1.0e-6 to 1.0e-8) are also tested and the numerical results show that further reduction of tolerances does not improve the accuracy of numerical results.

Accession Numbers

Sequence data from this article can be found in The Arabidopsis Information Resource (http://www.arabidopsis.org) data libraries under accession numbers: AT3G48090 (*EDS1*; https://www.arabidopsis.org/servlets/TairObject?id=39706&type=locus) and AT1G74710 (*ICS1*; https://www.arabidopsis.org/servlets/TairObject?id=28521&type=locus).

Supplemental Data

The following supplemental materials are available.

Supplemental Figure S1. Effects of K_{14}, the dissociation equilibrium constant for the binding of the Ca^{2+}–CaM complex to the *i*th TF, on gene expression regulated by the TF for calcium signature shown in this figure.

Supplemental Figure S2. Effects of K_{14}, the dissociation equilibrium constant for the binding of the Ca^{2+}–CaM complex to the *i*th TF, on gene expression regulated by the TF for calcium signature shown in this figure.

Supplemental Figure S3. Two calcium signatures are decoded to generate specific expression of *EDS1* and *ICS1* following the design principle:

responses of two active signals, $4Ca^{2+}$–CaM–CAMTA3 and $4Ca^{2+}$–CaM–CBP60g, to two experimentally measured calcium signatures.

Supplemental Table S1. Interactions of Ca^{2+}, CaM, and one TF.

Supplemental Table S2. Experimentally measured parameters for the interactions between Ca^{2+} and CaM.

Supplemental Text. Analysing design principle for decoding calcium signals to generate specific gene expression via transcription.

Received August 20, 2019; accepted October 31, 2019; published November 19, 2019.

LITERATURE CITED

Alberty RA (2004) Principle of detailed balance in kinetics. J Chem Educ **81:** 1206–1209

Allen GJ, Chu SP, Harrington CL, Schumacher K, Hoffmann T, Tang YY, Grill E, Schroeder JI (2001) A defined range of guard cell calcium oscillation parameters encodes stomatal movements. Nature **411:** 1053–1057

Aslam SN, Newman MA, Erbs G, Morrissey KL, Chinchilla D, Boller T, Jensen TT, De Castro C, Ierano T, Molinaro A, et al (2008) Bacterial polysaccharides suppress induced innate immunity by calcium chelation. Curr Biol **18:** 1078–1083

Atkinson NJ, Lilley CJ, Urwin PE (2013) Identification of genes involved in the response of Arabidopsis to simultaneous biotic and abiotic stresses. Plant Physiol **162:** 2028–2041

Bender KW, Zielinski RE, Huber SC (2018) Revisiting paradigms of Ca^{2+} signaling protein kinase regulation in plants. Biochem J **475:** 207–223

Bickerton PD, Pittman JKC (2012) Calcium signalling in plants. John Wiley & Sons, Chichester, UK, pp 1–9

Bouché N, Scharlat A, Snedden W, Bouchez D, Fromm H (2002) A novel family of calmodulin-binding transcription activators in multicellular organisms. J Biol Chem **277:** 21851–21861

Brophy JA, Voigt CA (2014) Principles of genetic circuit design. Nat Methods **11:** 508–520

Chubukov V, Zuleta IA, Li H (2012) Regulatory architecture determines optimal regulation of gene expression in metabolic pathways. Proc Natl Acad Sci USA **109:** 5127–5132

Clayton H, Knight MR, Knight H, McAinsh MR, Hetherington AM (1999) Dissection of the ozone-induced calcium signature. Plant J **17:** 575–579

Dodd AN, Kudla J, Sanders D (2010) The language of calcium signaling. Annu Rev Plant Biol **61:** 593–620

Edel KH, Marchadier E, Brownlee C, Kudla J, Hetherington AM (2017) The evolution of calcium-based signalling in plants. Curr Biol **27:** R667–R679

Fajmut A, Brumen M, Schuster S (2005) Theoretical model of the interactions between Ca^{2+}, calmodulin and myosin light chain kinase. FEBS Lett **579:** 4361–4366

Finkler A, Ashery-Padan R, Fromm H (2007) CAMTAs: Calmodulin-binding transcription activators from plants to human. FEBS Lett **581:** 3893–3898

Finn BE, Forsén S (1995) The evolving model of calmodulin structure, function and activation. Structure **3:** 7–11

Fromm H, Finkler A (2015) Repression and de-repression of gene expression in the plant immune response: The complexity of modulation by Ca^{2+} and calmodulin. Mol Plant **8:** 671–673

Galon Y, Nave R, Boyce JM, Nachmias D, Knight MR, Fromm H (2008) Calmodulin-binding transcription activator (CAMTA) 3 mediates biotic defense responses in Arabidopsis. FEBS Lett **582:** 943–948

Karin O, Swisa A, Glaser B, Dor Y, Alon U (2016) Dynamical compensation in physiological circuits. Mol Syst Biol **12:** 886

Karlebach G, Shamir R (2008) Modelling and analysis of gene regulatory networks. Nat Rev Mol Cell Biol **9:** 770–780

Kim MC, Chung WS, Yun DJ, Cho MJ (2009) Calcium and calmodulin-mediated regulation of gene expression in plants. Mol Plant **2:** 13–21

Kim YS, An C, Park S, Gilmour SJ, Wang L, Renna L, Brandizzi F, Grumet R, Thomashow MF (2017) CAMTA-mediated regulation of salicylic acid immunity pathway genes in Arabidopsis exposed to low temperature and pathogen infection. Plant Cell **29:** 2465–2477

Knight H, Trewavas AJ, Knight MR (1996) Cold calcium signaling in Arabidopsis involves two cellular pools and a change in calcium signature after acclimation. Plant Cell **8:** 489–503

Knight H, Trewavas AJ, Knight MR (1997) Calcium signalling in *Arabidopsis thaliana* responding to drought and salinity. Plant J **12:** 1067–1078

Kubota Y, Putkey JA, Waxham MN (2007) Neurogranin controls the spatiotemporal pattern of postsynaptic Ca^{2+}/CaM signaling. Biophys J **93:** 3848–3859

Kudla J, Batistic O, Hashimoto K (2010) Calcium signals: The lead currency of plant information processing. Plant Cell **22:** 541–563

Kudla J, Becker D, Grill E, Hedrich R, Hippler M, Kummer U, Parniske M, Romeis T, Schumacher K (2018) Advances and current challenges in calcium signaling. New Phytol **218:** 414–431

Kuriyan J, Konforti B, Wemmer D (2013) The Molecules of Life Physical and Chemical Principles: Physical Principles and Cellular Dynamics. Garland Publishing, New York

La Verde V, Dominici P, Astegno A (2018) Towards understanding plant calcium signaling through calmodulin-like proteins: A biochemical and structural perspective. Int J Mol Sci **19:** 19

Lenzoni G, Liu J, Knight MR (2018) Predicting plant immunity gene expression by identifying the decoding mechanism of calcium signatures. New Phytol **217:** 1598–1609

Linse S, Helmersson A, Forsén S (1991) Calcium binding to calmodulin and its globular domains. J Biol Chem **266:** 8050–8054

Liu J, Whalley HJ, Knight MR (2015) Combining modelling and experimental approaches to explain how calcium signatures are decoded by calmodulin-binding transcription activators (CAMTAs) to produce specific gene expression responses. New Phytol **208:** 174–187

Love J, Dodd AN, Webb AA (2004) Circadian and diurnal calcium oscillations encode photoperiodic information in Arabidopsis. Plant Cell **16:** 956–966

McAinsh MR, Pittman JK (2009) Shaping the calcium signature. New Phytol **181:** 275–294

McAinsh MR, Webb A, Taylor JE, Hetherington AM (1995) Stimulus-induced oscillations in guard cell cytosolic free calcium. Plant Cell **7:** 1207–1219

Medvedev SS (2018) Principles of calcium signal generation and transduction in plant cells. Russ J Plant Physiol **65:** 771–783

Miller JB, Pratap A, Miyahara A, Zhou L, Bornemann S, Morris RJ, Oldroyd GE (2013) Calcium/calmodulin-dependent protein kinase is negatively and positively regulated by calcium, providing a mechanism for decoding calcium responses during symbiosis signaling. Plant Cell **25:** 5053–5066

Miwa H, Sun J, Oldroyd GE, Downie JA (2006) Analysis of calcium spiking using a Cameleon calcium sensor reveals that nodulation gene expression is regulated by calcium spike number and the developmental status of the cell. Plant J **48:** 883–894

Pepke S, Kinzer-Ursem T, Mihalas S, Kennedy MB (2010) A dynamic model of interactions of Ca^{2+}, calmodulin, and catalytic subunits of Ca^{2+}/calmodulin-dependent protein kinase II. PLOS Comput Biol **6:** e1000675

Pifl C, Plank B, Wyskovsky W, Bertel O, Hellmann G, Suko J (1984) Calmodulin X $(Ca^{2+})4$ is the active calmodulin-calcium species activating the calcium-, calmodulin-dependent protein kinase of cardiac sarcoplasmic reticulum in the regulation of the calcium pump. Biochim Biophys Acta **773:** 197–206

Poovaiah BW, Du L, Wang H, Yang T (2013) Recent advances in calcium/calmodulin-mediated signaling with an emphasis on plant-microbe interactions. Plant Physiol **163:** 531–542

Purvis JE, Lahav G (2013) Encoding and decoding cellular information through signaling dynamics. Cell **152:** 945–956

Reddy AS, Ali GS, Celesnik H, Day IS (2011) Coping with stresses: Roles of calcium- and calcium/calmodulin-regulated gene expression. Plant Cell **23:** 2010–2032

Romano DR, Pharris MC, Patel NM, Kinzer-Ursem TL (2017) Competitive tuning: Competition's role in setting the frequency-dependence of Ca^{2+}-dependent proteins. PLOS Comput Biol **13:** e1005820

Salvador A, Savageau MA (2003) Quantitative evolutionary design of glucose 6-phosphate dehydrogenase expression in human erythrocytes. Proc Natl Acad Sci USA **100:** 14463–14468

Salvador A, Savageau MA (2006) Evolution of enzymes in a series is driven by dissimilar functional demands. Proc Natl Acad Sci USA **103:** 2226–2231

Savageau MA (2001) Design principles for elementary gene circuits: Elements, methods, and examples. Chaos **11:** 142–159

Seybold H, Trempel F, Ranf S, Scheel D, Romeis T, Lee J (2014) Ca^{2+} signalling in plant immune response: from pattern recognition receptors to Ca^{2+} decoding mechanisms. New Phytol **204:** 782–790

Shifman JM, Choi MH, Mihalas S, Mayo SL, Kennedy MB (2006) Ca^{2+}/calmodulin-dependent protein kinase II (CaMKII) is activated by calmodulin with two bound calciums. Proc Natl Acad Sci USA **103:** 13968–13973

Short EF, North KA, Roberts MR, Hetherington AM, Shirras AD, McAinsh MR (2012) A stress-specific calcium signature regulating an ozone-responsive gene expression network in Arabidopsis. Plant J **71:** 948–961

Tolla DA, Kiley PJ, Lomnitz JG, Savageau MA (2015) Design principles of a conditional futile cycle exploited for regulation. Mol Biosyst **11:** 1841–1849

Tsuda K, Somssich IE (2015) Transcriptional networks in plant immunity. New Phytol **206:** 932–947

Valeyev NV, Bates DG, Heslop-Harrison P, Postlethwaite I, Kotov NV (2008) Elucidating the mechanisms of cooperative calcium-calmodulin interactions: A structural systems biology approach. BMC Syst Biol **2:** 48

Virdi AS, Singh S, Singh P (2015) Abiotic stress responses in plants: Roles of calmodulin-regulated proteins. Front Plant Sci **6:** 809

Wall ME, Hlavacek WS, Savageau MA (2003) Design principles for regulator gene expression in a repressible gene circuit. J Mol Biol **332:** 861–876

Wang L, Tsuda K, Sato M, Cohen JD, Katagiri F, Glazebrook J (2009) Arabidopsis CaM binding protein CBP60g contributes to MAMP-induced SA accumulation and is involved in disease resistance against *Pseudomonas syringae*. PLoS Pathog **5:** e1000301

Wang L, Tsuda K, Truman W, Sato M, Nguyen V, Katagiri F, Glazebrook J (2011) CBP60g and SARD1 play partially redundant critical roles in salicylic acid signaling. Plant J **67:** 1029–1041

Whalley HJ, Knight MR (2013) Calcium signatures are decoded by plants to give specific gene responses. New Phytol **197:** 690–693

Whalley HJ, Sargeant AW, Steele JFC, Lacoere T, Lamb R, Saunders NJ, Knight H, Knight MR (2011) Transcriptomic analysis reveals calcium regulation of specific promoter motifs in Arabidopsis. Plant Cell **23:** 4079–4095

Yip Delormel T, Boudsocq M (2019) Properties and functions of calcium-dependent protein kinases and their relatives in *Arabidopsis thaliana*. New Phytol **224:** 585–604

Yuan P, Jauregui E, Du L, Tanaka K, Poovaiah BW (2017) Calcium signatures and signaling events orchestrate plant-microbe interactions. Curr Opin Plant Biol **38:** 173–183

Zhang L, Du L, Shen C, Yang Y, Poovaiah BW (2014) Regulation of plant immunity through ubiquitin-mediated modulation of Ca^{2+}-calmodulin-AtSR1/CAMTA3 signaling. Plant J **78:** 269–281

Zhang Y, Xu S, Ding P, Wang D, Cheng YT, He J, Gao M, Xu F, Li Y, Zhu Z, Li X, Zhang Y (2010) Control of salicylic acid synthesis and systemic acquired resistance by two members of a plant-specific family of transcription factors. Proc Natl Acad Sci USA **107:** 18220–18225

Zhu JK (2016) Abiotic stress signaling and responses in plants. Cell **167:** 313–324